The thermodynamics of clocks

G. J. Milburn

Taylor & Francis
Taylor & Francis Group

Check for updates

The thermodynamics of clocks

G. J. Milburn

Centre for Engineered Quantum Systems, School of Mathematics and Physics, The University of Queensland, Saint Lucia, Australia

ABSTRACT

All clocks, classical or quantum, are open non equilibrium irreversible systems subject to the constraints of thermodynamics. Using examples I show that these constraints necessarily limit the performance of clocks and that good clocks require large energy dissipation. For periodic clocks, operating on a limit cycle, this is a consequence of phase diffusion. It is also true for non periodic clocks (for example, radio carbon dating) but due to telegraph noise not to phase diffusion. In this case a key role is played by accurate measurements that decrease entropy, thereby raising the free energy of the clock, and requires access to a low entropy reservoir. In the quantum case, for which thermal noise is replaced by quantum noise (spontaneous emission or tunnelling), measurement plays an essential role for both periodic and non periodic clocks. The paper concludes with a discussion of the Tolman relations and Rovelli's thermal time hypothesis in terms of clock thermodynamics.

1. Introduction

A clock is a machine and like all machines subject to the laws of thermodynamics. In popular discussions, a clock is often presented as the epitome of a reversible and predictable dynamical system. Nothing could be further from the truth. As I will explain, a careful examination of the requirements for a clock indicates that a clock cannot be reversible and in fact requires dissipation for correct operation. I will use a number of examples, both classical and quantum, to illustrate this. I will also discuss irreversible clocks such as radio carbon dating and Mach's temperature clock. A unified description can be given by focusing on how clocks, as non equilibrium steady state systems, exploit sources of low entropy energy (high free energy).

There is a bewildering range of clocks, from biochemical to astronomical, from mechanical to stochastic, and it is difficult to give a general definition of a clock to cover all instances. A standard dictionary definition states 'a clock is a device to measure time', which begs a very much bigger and enduring question. Other definitions emphasise the repetitive or periodic nature of clock states, yet radio carbon dating is a clock that is anything but periodic as was the water clock used by Galileo.

I will take the view that a clock is a physical device used to coordinate local coincidences of physical events. This captures the central features of time in General Relativity; proper time is local and coordinates relationships between local physical events. Under this definition clocks can be used to plan ahead by referring to future coincidences, to sequence historical events (radio-carbon dating), or to synchronise events in different locations for navigation. This definition also shares some of the characteristics of distance measurements in enabling us to speak about 'here and now'. If clocks do measure time, this definition captures the relational character of time: for three localised events, if event C happens at the same time as A and B then A happens at the same time as B. The similarity to the zeroth law of thermodynamics is not coincidental.

In order to use a physical system to coordinate coincidences, we count the number of times a recurring physical event is observed to occur in the clock between coincident events happening here and now and coincident events here and in the future. We can add to the basic clock a device that keeps the count and displays the number. Clocks are all about counting. Woods [1] refers to this type of clock as a *ticking clock* to distinguish from a device that simply measures the elapsed time between two fixed events, a *stopwatch*. The important distinction identified by Woods rests on the distinction between the requirement to make repeated measurements on a ticking clock and a single measurement in respect of a stopwatch. In a ticking clock continuous observations are central

---

CONTACT G. J. Milburn ✉ milburn@physics.uq.edu.au

to its operation. For classical clocks this is not necessarily a significant distinction but for quantum clocks it certainly is.

Length measurements are also about counting: count the number of times a ruler is placed, end to end, between one point and another. Good rulers are those systems that do not change their length when used in this way. If they did change, it would cause the count to vary for repeated measurements of the same distance. Likewise, good clocks are those for which the number of counts between periodic coincidences does not fluctuate. Of course in reality there is no perfect ruler; depending on the material used the length of the ruler could fluctuate a little or a lot. Likewise, there is no perfect clock. How good a ruler or a clock needs to be depends on the nature of the physical events that we seek to coordinate.

2. The essential irreversible character of periodic clocks

I will begin with periodic clocks. As any rudimentary textbook on clocks will describe [2], the simplest such devices are driven, periodic systems, perhaps stabilised by feedback and with some counting mechanism to track the number of repetitions of a periodic variable.

The pendulum clock with the escapement mechanism revolutionised the mechanical clock following its invention by Huygen's in 1656. It comprises a pendulum that, for small oscillations in the absence of dissipation, will oscillate at constant amplitude and frequency (the natural frequency) determined by its length and acceleration due to gravity. But a pendulum once set in motion will eventually stop oscillating due to friction between the support and the rod, collisions with air molecules or other uncontrollable interactions with the environment. To sustain an oscillation the pendulum must be driven and this is the role of the escapement in early pendulum clocks.

The purpose of the escapement mechanism is to input energy to the pendulum to counteract the effects of dissipation. With careful design, the driven pendulum will settle into a steady oscillation at or close to its natural frequency. We refer to this sustained oscillation as a limit-cycle; a stable steady state of sustained oscillatory motion. Limit cycles are common in driven, dissipative non linear systems. Dissipative attractors, such as a limit cycle, ensure clocks based on this phenomenon are necessarily stochastic dynamical systems; a necessary consequence of the fluctuation-dissipation theorem [3].

2.1. Dissipation and noise in the escapement pendulum clock

A pendulum, for small oscillations, is a linear dynamical system so how can a limit cycle occur? It is the driving
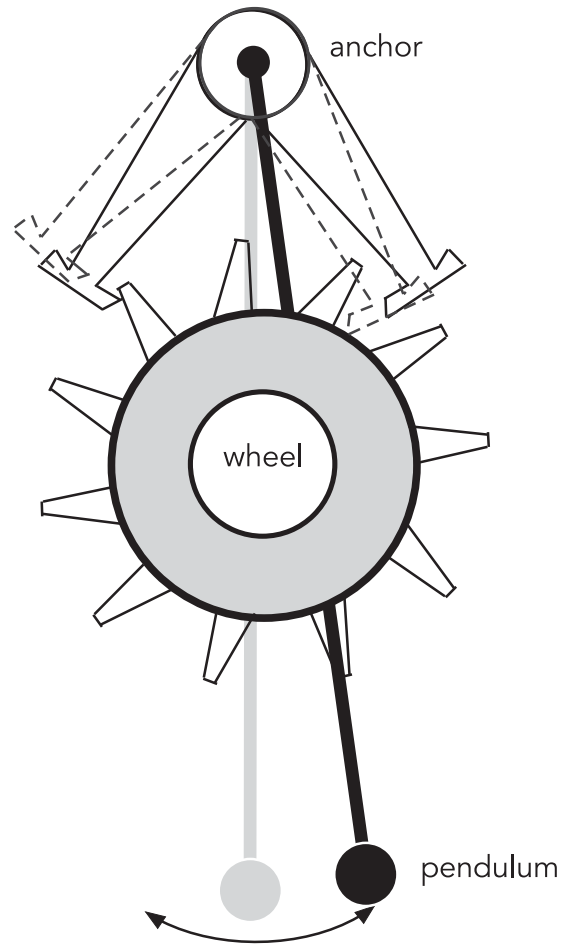

Figure 1. A schematic anchor and escape wheel. The falling mass that provides a constant torque to the wheel is not shown. As the pendulum unlocks the anchor from its right hand or left hand position, it imparts a small impulsive torque to the pendulum. The sequence is: left-lock → clockwise kick → free → right-lock → anticlockwise kick → free → left-lock. Initial transients are not shown.

mechanism of the escapement itself that is responsible for the non linearity. The magnitude of the impulse delivered depends non linearly on the angular displacement and possibly the angular velocity. Non linearity is central to clock design. I will use the Graham escapement mechanism as an example [4, 5] schematically indicated in Figure 1 based on the 'wheel and anchor' mechanism.

I will adapt the treatment of [6] to a Hamiltonian phase-space description. For a pendulum the phase space variables are angular displacement, θ, and the angular momentum, p. When dissipation and fluctuations are included Hamilton's equations are modified to become Langevin equations. In this case,

$$\dot{\theta} = \frac{p}{m\omega l} \tag{1}$$

$$\dot{p} = -mg\theta - \gamma p + K(\theta, p) + \xi(t) \tag{2}$$

where the · indicates a time derivative, m is the mass, $\omega = \sqrt{g/l}$ is the natural frequency of the pendulum of length l and γ is the frictional damping rate. The fluctuating force term $\xi(t)$ is a white noise process of mean zero and (stationary) two-time correlation function $\overline{\xi(t)\xi(t+\tau)} = D\delta(\tau)$. The fluctuation-dissipation theorem requires $D = 2m\gamma k_B T$. The term $K(\theta, p)$ describes small impulsive kicks delivered by the design of the escapement [6].

It is simpler to move to dimensionless variables defined by $x = \theta$ and $y = p/(m\omega l)$ and a dimensionless time $\tau = \omega t$, so that the equations take the form

$$\dot{x} = y \tag{3}$$

$$\dot{y} = -x - \Gamma y + K(x, y) + \eta(t) \tag{4}$$

where $\Gamma = \frac{\gamma}{m\omega^2 l}$ and $\eta(t) = \frac{\xi(t)}{m\omega^2 l}$. For the kicks we take

$$K(x, y) = -\mu \, \text{sign}(\sin\psi_0 \, x - \cos\psi_0 \, y) \tag{5}$$

where ψ_0 is fixed by the design of the escapement and μ has units of frequency. This is a non linear function of the phase space variables. Note that as we are using the quadratic approximation for the pendulum potential function we need to ensure that $x_0 \ll \pi/2$. We can easily remove this approximation, see [6]. A phase-space picture of this impulse is shown in Figure 2. It provides constant kick to the momentum once every half period.
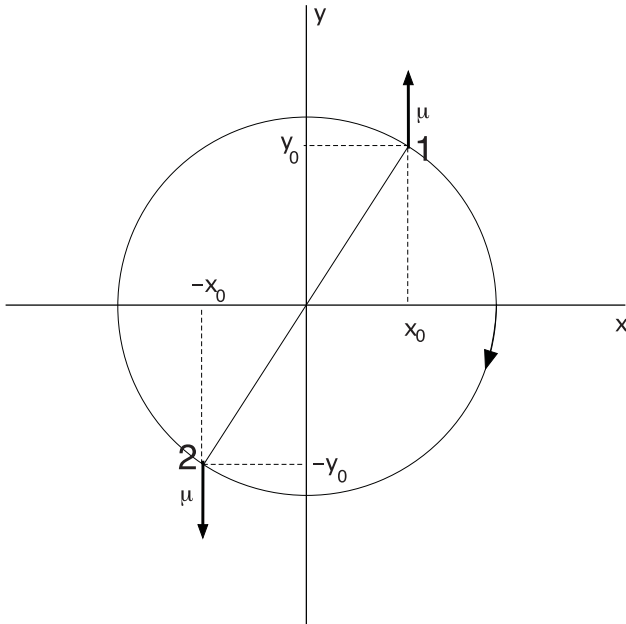

Figure 2. A phase-space representation of momentum kicks provided to the pendulum every half cycle by the escapement mechanism with $\tan\psi_0 = y_0/x_0$. At point labelled 1, the impulse switches $-\mu \to +\mu$ while at point labelled 2 the impulse switches $+\mu \to -\mu$.
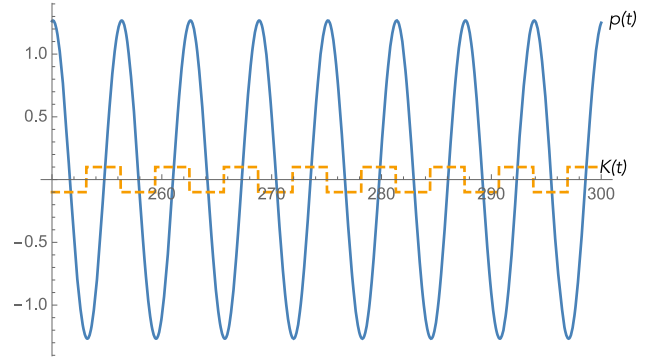

Figure 3. The angular displacement (solid) and the impulse function (dashed) as a function of time for the kicked pendulum with $\sin\psi_0 = 0.1$ $\Gamma = 0.1$ $\mu = 0.1$.

In Figure 3 we plot the dimensionless momentum, y, as a function of time together with the impulse function $K(x, y)$, in units where $\mu = 1$. The stable limit cycle is apparent.

In order to extract the limit cycle, define new variables, r, ψ, by $x = r\cos\psi$ and $y = r\sin\psi$. The time scale of the decay onto the limit cycle (the $r(t)$ dynamics) is slower than the oscillation frequency on the limit cycle (the $\psi(t)$ dynamics). This implies that we can average over the oscillatory faster time scale which is equivalent to averaging over ψ from $-\pi - \psi_0$ to $\pi - \psi_0$, the equation for the radial coordinate after averaging is

$$\dot{r} = -\frac{\Gamma r}{2} + \frac{2\mu}{\pi}\cos\psi_0 \tag{6}$$

It is now clear that there is a stable fixed point in the radial coordinate given by,

$$r_* = \frac{4\mu}{\pi\Gamma}\cos\psi_0 \tag{7}$$

The dynamics for the phase is

$$\dot{\psi} = -1 + \frac{2\mu}{r\pi}\sin\psi_0 \tag{8}$$

The frequency is shifted from that of the free oscillator and only approaches the free oscillator in a limit such that the size of the impulsive kicks goes to zero.

In scaled units we define the energy of the oscillator as

$$E = \frac{1}{2}(x^2 + y^2) = \frac{1}{2}r^2 \tag{9}$$

If we time-average this over the fast oscillations on the limit cycle we find that

$$\dot{E} = -\Gamma E + \frac{2\sqrt{2E}\mu}{\pi}\cos\psi_0 \tag{10}$$

The last term is the average rate at which work is done by the escapement on the pendulum. The limit cycle forms

when the energy lost due to friction is balanced by the work done by the escapement. The important feature is that the work done increases with the size of the limit cycle. In the steady state, the average energy on the limit cycle is

$$\overline{E} = \frac{8\mu^2}{\Gamma^2 \pi^2} \cos^2 \psi_0 \tag{11}$$

Of course this result depends on the assumption that the dynamics is deterministic; noise is neglected.

A dynamical system subject to dissipation must necessarily experience noise. This is a direct consequence of the fluctuation-dissipation theorem [3, 7]. As a primer, consider Equation (3) with no deterministic applied force, K, only a stochastic applied force, $\eta(t)$. The assumption that these forces are delta correlated is of course an approximation based on the vastly different time scales on which system and bath correlation functions decay. However this assumption introduces a peculiar mathematical problem that requires special attention. A delta correlated fluctuating force has infinite variance which no physical fluctuating force can have. Physically we require that both $x(t), y(t)$ are continuous functions of time so that one expects that the integral

$$W(t) = \int_0^t \mathrm{d}t' \xi(t') \tag{12}$$

is a physically meaningful continuous quantity: It corresponds to a diffusion process, that is to say, it has a mean square that increases linearly in time. Unfortunately it is not differentiable as the mean *square* of $\mathrm{d}W(t) = W(t + \mathrm{d}t) - W(t)$ is only linear in dt. (See Section 3.8 of [8]). Despite this $W(t)$ is a physically meaningful quantity so long as we can correctly interpret integrals of the form $\int f(t) \, \mathrm{d}W(t)$. The problem thus reduces to a question of defining stochastic integration. There are two choices that are usually made: Stratonovich and Ito. The details are not relevant here (see [8]). I simply note that the Ito interpretation of the integral leads to considerably simpler calculations of moments but at a price: the rules of calculus need to be changed to reflect that the average of $\mathrm{d}W(t)^2$ is in fact linear in $\mathrm{d}t$. To summarise; while equations of the form Equations (3) are problematic, the incremental form

$$\mathrm{d}x = y \, \mathrm{d}t \tag{13}$$

$$\mathrm{d}y = -x \, \mathrm{d}t - \Gamma y \, \mathrm{d}t + \sigma \, \mathrm{d}W(t) \tag{14}$$

(with $\sigma^2 = 2m\Gamma k_B T$) are meaningful provided we know the definition of the integral of a stochastic function.

For example, suppose we seek to find an equation of motion for the energy $E = (x^2 + y^2)/2$. The rules of regular calculus would imply that

$$\mathrm{d}E = \mathrm{d}x.x + \mathrm{d}y.y \tag{15}$$

Using Equations (13)

$$\mathrm{d}E = -\Gamma y^2 \, \mathrm{d}t + \sigma y. \, \mathrm{d}W(t) \tag{16}$$

Taking the average this shows that the rate of change of the average energy decays to zero. This is inconsistent with the equipartition theorem which says that the steady state average of the energy is proportional to kT, that is to say, σ. However the Ito calculus requires that we take

$$\mathrm{d}E = \mathrm{d}x.x + \mathrm{d}y.y + (\mathrm{d}x^2 + \mathrm{d}y^2)/2 \tag{17}$$

We must now keep terms in $\mathrm{d}W(t)^2$ as on averaging these are proportional to $\mathrm{d}t$. This gives for the rate of change of average energy

$$\frac{\mathrm{d}\overline{E}}{\mathrm{d}t} = -\Gamma \overline{y^2} + \frac{\sigma^2}{2} \tag{18}$$

Thus in the steady state the mean square average of momentum is

$$\overline{y^2} = \frac{\sigma^2}{2\Gamma} \tag{19}$$

Using the dimensioned momentum variable this is equivalent to $\overline{p^2} = m k_B T$. Thus the average kinetic energy in the steady state is equal to $k_B T/2$ as required.

In the case of nonlinear systems, the inclusion of white noise and the need to distinguish the Ito and Stratonovich descriptions requires special care. The nonlinear transformation to radial and phase variables leads to non linear noise in both $\dot{r}, \dot{\psi}$. I will simply quote the result in [9] for Ito stochastic differential equations after phase averaging,

$$\mathrm{d}r = \left[-\frac{\Gamma r}{2} + \frac{2\mu}{\pi} \cos \psi_0 + \frac{D'}{4r} \right] \mathrm{d}t + \sqrt{D'/2} \, \mathrm{d}W_1(t) \tag{20}$$

$$\mathrm{d}\psi = \left[-1 + \frac{2\mu}{r\pi} \sin \psi_0 \right] \mathrm{d}t + \frac{\sqrt{D'/2}}{r} \mathrm{d}W_2(t) \tag{21}$$

where $\mathrm{d}W_1(t), \mathrm{d}W_2(t)$ are independent Wiener increments (random variables with zero mean and variance $\mathrm{d}t$) and the diffusion constant D' is given in terms of the dimensional diffusion constant D as

$$D' = \frac{D\omega}{m^2 g^2} = \frac{2\omega\gamma k_B T}{mg^2} \tag{22}$$

Further details on stochastic differential equations, Wiener increments and transforming from Langevin equations to Ito equations may be found in [8].

Two important effects are apparent: a small shift in the the radial fixed point and a non linear diffusion in the phase. The radial fixed point is changed to

$$r_* = \frac{2\mu}{\pi\Gamma}\cos\psi_0 + \sqrt{\frac{4\mu^2}{\pi^2\Gamma^2}\cos^2\psi_0 + D'/4} \quad (23)$$

We can linearise the effect of phase noise by setting setting $r \to r_*$ in the stochastic term for $d\psi$. This leads to the significant fact that the phase diffusion gets slower the larger the limit cycle. For typical pendulum clocks run at room temperature the phase diffusion rate is very small indeed and it is no surprise that this fundamental source of noise is not at all significant for such clocks.

However there are cases, especially for quantum clocks, where the phase noise on the limit cycle does limit the performance of the clock. The analysis begins by linearising the noise when the clock has settled onto the limit cycle.

2.2. Noise and period fluctuations

To understand the effect of noise it is useful to write the kick function directly in terms of the phase variable on the limit cycle as

$$K(t) = -\mu \, \text{sign}[\cos(\psi(t) + \psi_0)] \quad (24)$$

In the deterministic case, $\psi(t) = \tilde{\omega}t$ and this function is periodic on $-\pi/2 - \psi_0$ to $3\pi/2 - \psi_0$. The transitions between $\pm\mu$ occur at regular intervals separated in time by $\pi/\tilde{\omega}$. As the noise adds a random Gaussian variable to $\psi(t)$ over time t, these transitions become irregular; some a little early, some a little late. This suggests that the function $K(t)$ is developing the characteristics of a random telegraph signal (RTS). However it cannot be a simple RTS with constant transition rates as the transitions are most likely to occur at particular moments in
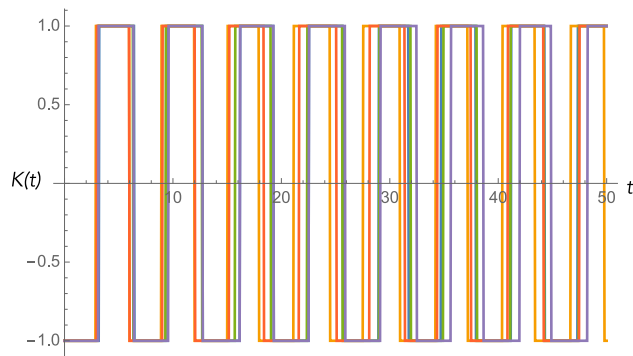
time near the end points of the oscillation. In Figure 4 I show five sample trajectories obtained by solving the Ito stochastic differential equation for the phase on the limit cycle

$$d\psi(t) = -\tilde{\omega}dt + \frac{\sigma}{r_*}dW(t) \quad (25)$$

and evaluating $K(t)$. The fluctuations in the switching times are clear.

Expanding the sign function in a Fourier series, the ensemble average of the $K(t)$, with $\psi_0 = 0$, on the limit cycle can be shown to be given by

$$E(K(t)) = \frac{4\mu}{\pi}\sum_{k=1}^{\infty} e^{-\sigma^2 t(2k-1)^2/(2r_*^2)}\frac{\sin((2k-1)\tilde{\omega}t)}{2k-1} \quad (26)$$

In Figure 5 I plot the ensemble average computed from 100 trials of the process shown in Figure 4 as well as the analytical expression given in Equation (26).

To estimate how the noise impacts the time keeping, fix the interval of external time that passes as T and ask how many 'ticks' of the clock occur in this time. In the clock literature this approach is known as time domain characterisation, as opposed to the frequency domain where the emphasis is on noise power spectral density [10]. The escapement force can be used to monitor this count. Each cycle of the square wave kick function corresponds to one tick of the clock. If there were no noise, a count of M cycles corresponds to a period in conventional time units of T/M. But in the presence of noise the count M and thus the assigned period fluctuates from one cycle to the next. Alternatively one can sample the time for one cycle, that is to say the period T, over many trials. In Figure 6 I plot a histogram distribution of this period in 500 trials for three different value of the noise level. The zero noise case gives a period of 6.35 which is the correct value for these parameters.
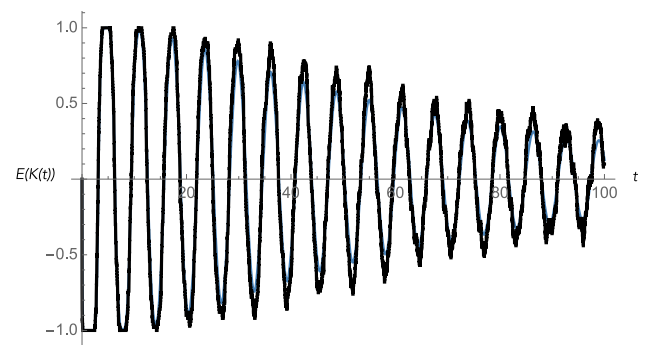

Figure 4. A plot of five sample trajectories of $K(t)$ with phase diffusion as a function of t with $\sin(\psi_0) = 0.1$, $\mu = \Gamma = 1.0$ and $\sigma = 0.1$.

Figure 5. The ensemble average over 100 samples of the process $K(t)$ as a function of t with $\psi_0 = 0$, $\tilde{\omega} = 1$, $\mu = \Gamma = 1.0$ and $\sigma = 0.2$. Also shown is the analytic expression given in Equation (26).
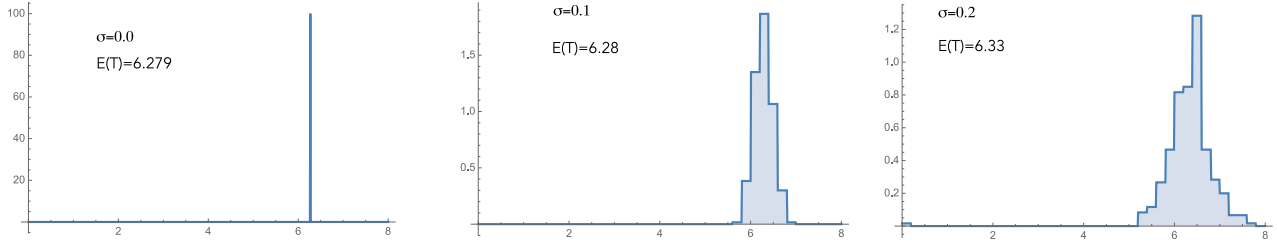
Figure 6. A histogram distribution of the same cycle of $K(t)$ over 300 trials with $A = 0.0$, $\gamma = 0.1$, $\mu = 0.1$, $\omega = 1.0$. Values for the mean period is $E(T)$.

In this linearised noise treatment it remains the case that the energy on the limit cycle does not change. However the work done by the escapement and hence the energy lost to friction fluctuates from one cycle of the escapement to the next. To see this observe that it follows from the equations of motion that the work, W, done by the escapement occurs at the rate $K(x, y)y$. Let one cycle of the clock start with a switch from $K = -\mu$ to $K = +\mu$. The work done by the escapement over one cycle is

$$W = \mu r_* \left[\int_{\tau_+} \sin(\psi(t))\, dt + \int_{\tau_-} |\sin(\psi(t))|\, dt \right]$$

(27)

where $\tau_\pm$ is the time spent in the state $K = \pm\mu$. As these intervals are random variables the work done in each cycle is a random variable. The heat dissipated on each is given by cycle $Q = W/\Gamma$, so fluctuations in W correspond to fluctuations in the heat dissipated. Putting it together, there is a relationship between fluctuations in the clock period and the fluctuations in the heat dissipated by the clock.

In the deterministic case the work done averaged over each cycle is related to the period by

$$W = \left(\frac{2\mu r^* \cos \psi_0}{\pi} \right) T$$

(28)

A simple estimate of the average heat dissipated per cycle is

$$Q = \left(\frac{2\mu r^* \cos \psi_0}{\pi \Gamma} \right) T$$

(29)

Including noise we expect both Q and T to fluctuate from one cycle to the next.

In Figure 7 I plot the result of 50 simulations for the work done on the first half cycle versus the corresponding period. The work done is computed numerically from the integral

$$W_k = \mu r^* \int_0^{T_k/2} dt \sin \psi(t))$$

(30)

by numerically solving the Ito stochastic differential equations for $d\psi(t)$ using the Ito solver in Mathematica.
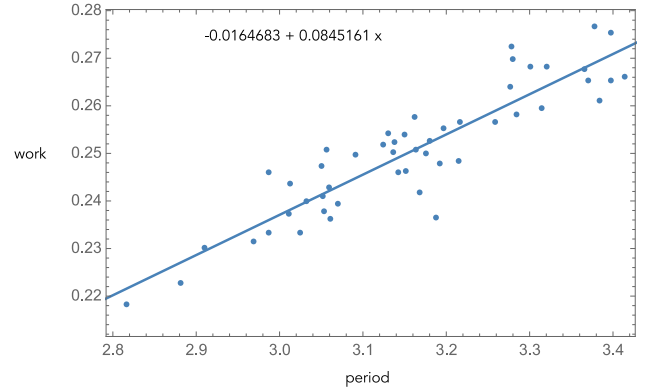

Figure 7. A plot of the work done versus period for the first half cycle in 50 sample trajectories with $\sin \psi_0 = 0.2$, $\gamma = 0.1$, $\mu = 0.1$, $\omega = 1.0$, $\sigma = 0.1$. The linear fit is $-0.0164683 + 0.0845161x$.

A linear fit indicates a slope of 0.085 while Equation (28) for these parameters gives a slope of 0.078.

The fluctuations in Q thus determine the fluctuations in the period and thus the quality of the clock. Noting that the fluctuations in the period depend on the phase diffusion noise and this scales inversely with the size of the limit cycle r_*, while the average heat lost per cycle scales with the size of the limit cycle, the more accurate the clock the greater is the heat dissipated. This important thermodynamic constraint on the accuracy of clocks was first presented by Erker at al. [11] in the context of an abstract quantum model. We see here it is a consequence of the dissipative nature of a simple classical periodic clock. It also follows that on the limit cycle $Q/T = 4\mu r_*$, a constant on all cycles. This implies that the fractional error in heat dissipated and clock frequency are related by

$$\frac{\delta Q}{Q} = \frac{\delta \omega}{\omega}$$

(31)

A similar result occurs in the context of non periodic thermal clocks as I discuss in Section 4. In Section 3 I will consider quantum periodic clocks. There the noise on the limit cycle arises from a fundamental quantum sources of noise: spontaneous emission and quantum tunnelling. These processes do not go to zero at zero temperature and
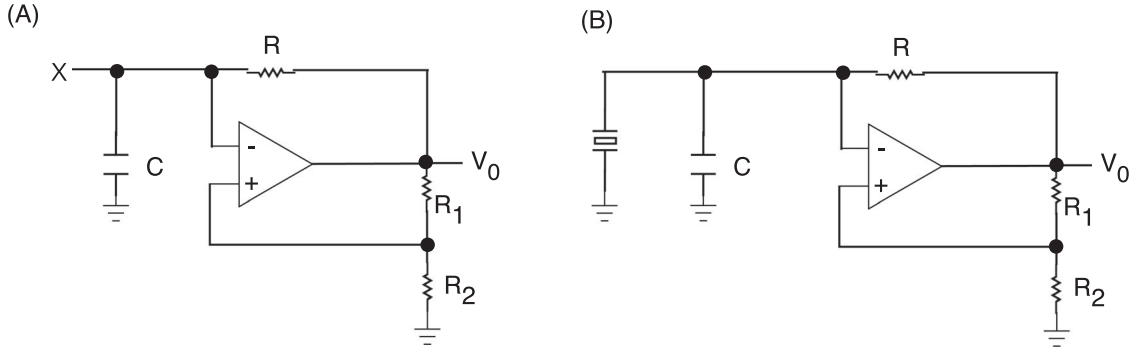
Figure 8. (a). A Schmidtt trigger Op Amp. with feedback configured as an astable oscillator (b) A quartz piezo electric oscillator coupled to an astable oscialltor.

thus quantum thermodynamics limits the accuracy of all clocks.

2.3. Dissipation and noise in the quartz oscillator clock

As a second example of a well known periodic clock I will consider the electronic quartz oscillator clock. A shortcoming of the treatment of the escapement pendulum clock in the previous section is the omission of the back-action of the pendulum on the escapement: the kick function was simply imposed. The quartz oscillator clock gives an opportunity to move beyond this. The two key discoveries that led to the quartz clock are; the discovery of relaxation oscillations (another name for limit cycles) in vacuum tube circuits and the high quality piezo-electric oscillations exhibited by small crystals of quartz. A good summary of the history is given by the inventor, Warren Marrison [12].

I will focus here on the relaxation oscillations exhibited in a feedback circuit to form a Schmidtt trigger. A typical Schmidtt trigger has the circuit diagram shown in Figure 8(a). The Op Amp is configured as a comparator. The input voltage is applied at the inverting input. The non inverting input voltage is determined by a voltage divider comprised of resistors R_1, R_2. The initial output of the Op Amp, V_0, is at the saturation voltage V_s. The voltage at the + terminal is βV_s where $\beta = R_1/(R_1 + R_2)$. If the input voltage at the − terminal ramps up from a low value and exceeds βV_s, the output switches to $-V_s$. Now ramping the voltage at the − terminal back down, the output will switch back to $+V_s$.

A phenomenological model for the Schmidtt trigger is given by the equation

$$\dot{V} = \gamma(1 - g(V))e^{-\eta X} - \gamma(1 + g(V))e^{\eta X} \quad (32)$$

where V is the output voltage and X is the applied voltage at the inverting terminal. The exponential dependence on

voltage, X, reflects an avalanche-like switching between reverse and forward biased transistors inside the device. At steady state for fixed X, the system rapidly decays onto the steady state output voltage V_{ss} as a function of the input X given implicitly by

$$g(V_{ss}) = -\tanh(\eta X) \quad (33)$$

Clearly $|g(V_{ss})| \leq 1$. In the case of a Schmidtt trigger built from an OP Amp with feed back as in Figure (5A)

$$g(V) = \frac{V + \tanh \beta V}{1 + V \tanh \beta V} \quad (34)$$

where $\beta = AR_2/(R_1 + R_2)$, and A is a parameter that determines the quality of the Op. Amp. Typically $A >> 1$. This is equivalent to the model discussed in reference [13].

Substituting Equation (33) into Equation (34) we can find X as a function of V,

$$X = -\frac{\beta}{\eta}V + \frac{1}{2\eta} \ln\left(\frac{1 + V}{1 - V}\right) \quad (35)$$

The turning points of $X(V)$ are given by $V_c = \pm\sqrt{\frac{\beta-1}{\beta}}$. The steady state response in shown in Figure 9 for the case $\beta = 1.8, \eta = 0.6$. The required hysteretic response of a Schmidtt trigger is evident.

When we include the quartz oscillator as shown in Figure 8(b), the input voltage to the Schmidtt trigger is the voltage on the equivalent capacitor of the quartz oscillator. The equations of motion become,

$$\dot{V} = \gamma(1 - g(V))e^{-\eta X} - \gamma(1 + g(V))e^{\eta X} \quad (36)$$

$$\dot{X} = \omega Y \quad (37)$$

$$\dot{Y} = -\omega X - \kappa Y + \chi V \quad (38)$$

where V is the output voltage of the Schmidtt trigger, X is the voltage on the equivalent circuit capacitor and Y is the
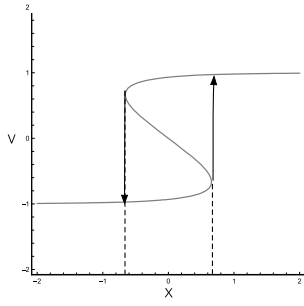
Figure 9. Two steady state response functions for a Schmidtt trigger output voltage as a function of the input voltage X. $\beta = 1.8, \eta = 0.6$.

flux in the equivalent circuit inductor for the quartz crystal and ω is the natural frequency of the equivalent LC circuit. The saturation voltage is set to unity. This is not a Hamiltonian system as there are only three equations. This is justified by the large dissipative time constant for the Schmidtt trigger.

A typical limit cycle trajectory for V and X are shown in Figure 10. The limit cycle occurs via a Hopf bifurcation for values of χ above a critical value where the fixed point at the origin becomes unstable. Comparing this to the treatment of the escapement clock in the previous section, it is easy to see how this system may be configured as a clock by a simple mechanism to count the number of transitions of the output voltage of the Op Amp.

On the limit cycle, $g(V(t)) = -\tanh(\eta x(t))$ from which it follows that $V(t) = -\tanh(\beta V(t) + \eta x(t))$. Substituting into the equation of motion for Y,

$$\dot{Y} = -\omega X - \kappa Y - \chi \tanh(\beta V + \eta x) \qquad (39)$$

$$\approx -\omega X - \kappa Y - \chi \,\mathrm{sign}(x) \qquad (40)$$
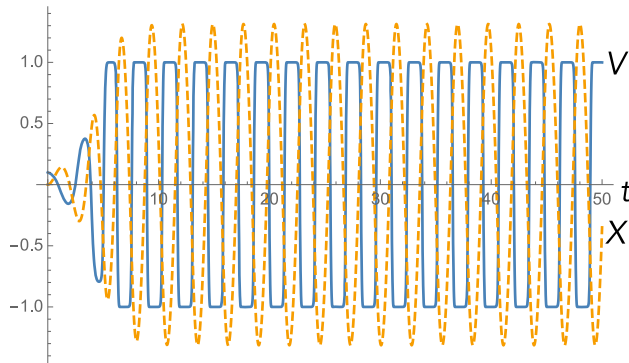

Figure 10. The limit cycle trajectories of the Schmidtt trigger output voltage (solid) and the voltage on the quartz crystal (dashed). The parameters are $\omega = 1, \gamma = 0.1, \eta = 8.0, \kappa = 1.0, \beta = 1.0$ and $\chi = 5.0$.

where the approximation becomes better in the limit that $\eta >> \beta > 1$ (noting that $|V(t)| \leq 1$). So this model reduces to the kick-function model discussed in the previous section.

Noise enters this description in the form of Johnson-Nyquist noise in Ohmic resistance. A phenomenlogical model of a Schmidtt trigger subject to thermal noise is presented in [13]. In the model used here this corresponds to adding a fluctuating white noise term to the equation of motion for X,

$$\dot{Y} = -\omega X - \kappa Y + \chi V + \sqrt{D}\,\mathrm{d}W(t) \qquad (41)$$

where D is a thermal diffusion constant and $\mathrm{d}W(t)$ is the Wiener process. The analysis proceeds much as in the previous example. After transients have died out the limit cycle can be described by using the variables (r, ψ). Linearising the noise on the limit cycle gives a constant phase diffusion. The implications for the accuracy of the clock are unchanged: the more energy is dissipated, the better the clock.

3. Quantum periodic clocks

3.1. Lasers

In atomic clocks the primary oscillator is an electric dipole non linear oscillator between a ground and excited state of an atom, although an ensemble of atoms is typically used. If the energy difference between the ground and excited state is ϵ, the resonance frequency of the atomic oscillator is $\omega = \epsilon/\hbar$. The driving system, playing the role of the escapement in a mechanical clock, is a laser. The electric field of the laser drives the atomic dipole transition. The coupling between the laser and the atomic oscillator can be made in various ways including a direct coupling or a feedback coupling; a distinction that Levine [14] refers to as active versus passive respectively. In atomic clocks both the drive oscillator and the atomic oscillator are nonlinear.

I will begin with the laser which, as Wiseman has cogently argued, is already a clock [15], albeit at a very high frequency. It converts a continuous (but stochastic) source of input energy, the 'pump', into a coherent oscillation at a (almost) fixed frequency provided the pump power is above a critical threshold. There is an irreducible level of quantum noise in the laser oscillator above threshold due to spontaneous emission.

The quantum theory of the laser is well established. Although there are a very large variety of lasers I will adopt one model for definiteness: an optical cavity containing a large number of atoms with an atomic transition close to the cavity frequency. A source of incoherent radiation, the 'pump', maintains a population inversion

between the ground and excited state of the transition (i.e. on average, more atoms are in the excited state than the ground state).

In a competition between the incoherent pumping and loss due to spontaneous and stimulated emission from the laser transition and the optical cavity, the electric field inside the cavity can reach a non equilibrium steady state. This steady state can undergo a non equilibrium phase transition as the pumping is increased above a threshold. Below the threshold the field is Gaussian distributed with average field amplitude of zero. Above the threshold, the field is non-Gaussian with a well defined intensity (Poisson distributed) and slowly diffusing phase with respect to the cavity frequency. In a semi-classical approach this transition is described as fixed point to limit cycle bifurcation with added noise.

I will base my discussion on the case in which the cavity loss dominates over atomic decay. In this case the gain medium can be adiabatically eliminated. A good discussion can be found in [16] and I will follow that approach.

A laser is the standard example of an open quantum systems driven far from thermal equilibrium so it might be helpful if I give some background on open quantum systems. I will begin with an empty single mode optical cavity. The quantum state of the intracavity field can be written in the photon number basis $|n\rangle$. We define annihilation and creation operators $a, a^\dagger$ by $a|n\rangle = \sqrt{n}|n-1\rangle$, $a^\dagger|n\rangle = \sqrt{n+1}|n+1\rangle$. It then follows that $a^\dagger a|n\rangle = n|n\rangle$. We call $a^\dagger a$ the photon number operator. If at some time the state of the field in the cavity is described by a general mixed state density operator, $\rho(t)$, the probability that the cavity contains n photons is $p_n(t) = \langle n|\rho(t)|n\rangle$. The mean number of photons in the cavity is then given by $\bar{n} = \sum_n np_n \equiv \langle a^\dagger a\rangle$.

In the laboratory frame the average cavity field oscillates at the cavity frequency ω_c. The first step is to move to the interaction picture at the cavity frequency which removes the average field oscillation altogether.

In order to model decay, I will assume that photons leak from the cavity at a constant rate κ. This means that emission is a Poisson point process; in a small interval of time from t to $t + dt$ either no photons are emitted or one and only one photon is emitted. The probability for a single photon to be emitted in a small interval of time t to $t + dt$ is $p(1; t) = \kappa p_n(t) \, dt = \kappa \langle a^\dagger a\rangle \, dt$. In most time intervals dt however no photons are emitted and the probability for this to happen is clearly $p(0; t) = 1 - p(1; t)$.

How does the state of the cavity field change when one photon is emitted? Whatever it is it must have one photon less so we can describe it in terms of the annihilation operator as the (unnormalised) conditional state

$\rho^{(1)}(t) = a\rho(t)a^\dagger$. One might think that if no photons are emitted the state is unchanged but that can't be right. If no photons are emitted it may be the case there were no photons to begin with. If you keep seeing nothing for a long period of time it is becoming increasingly likely that indeed there are no photons to emit. In other words not seeing something is still providing information on the state of the system and thus the probability assignments need to be updated.

We can update the state $\rho(t)$ to $\rho(t + dt)$ in terms of a mixture of the two events that can happen: emission and no emission. It turns out that the correct updating is done as

$$\rho(t + dt) = \kappa a\rho(t)a^\dagger \, dt + [1 - \kappa a^\dagger a \, dt]\frac{\rho(t)}{2}$$
$$+ \frac{\rho(t)}{2}[1 - \kappa a^\dagger a \, dt] \qquad (42)$$

where the last two terms are the updating required for not seeing an event. Note that the trace of the first term is just $p(1; t)$ while the trace of the remaining term is $p(0; t) = 1 - p(1; t)$. It is now a simple matter to rearrange this equation to give the master equation

$$\frac{d\rho}{dt} = \kappa a\rho a^\dagger - \frac{\kappa}{2}(a^\dagger a\rho + \rho a^\dagger a) \equiv \kappa \mathcal{D}[a]\rho \qquad (43)$$

where I have defined a super operator $\mathcal{D}[A]\rho = A\rho A^\dagger - \frac{1}{2}(A^\dagger A\rho + \rho A^\dagger A)$. Equation (43) is the master equation describing an open empty cavity without driving. The equation of motion for the mean photon number $\langle a^\dagger a\rangle = \text{tr}(a^\dagger a\rho)$ is then found to be

$$\frac{d\langle a^\dagger a\rangle}{dt} = -\kappa \langle a^\dagger a\rangle \qquad (44)$$

The argument can equally well be run for the case in which photons are injected into the cavity at constant rate γ. It is easy to see that in this case the master equation is

$$\frac{d\rho}{dt} = \gamma \mathcal{D}[a^\dagger]\rho \qquad (45)$$

The mean photon number then satisfies

$$\frac{d\langle a^\dagger a\rangle}{dt} = \gamma\left(\langle a^\dagger a\rangle + \frac{1}{2}\right) \qquad (46)$$

The 'plus half' term implies that the cavity will be excited from the vacuum state by such an amplifier.

Phase diffusion is another case in which a simple argument leads to the correct master equation. Suppose that at Poisson distributed times the system is subject to a unitary transformation of the form

$$\rho \to U(\theta)\rho U^\dagger(\theta) \qquad (47)$$

with $U(\theta) = e^{-i\theta a^\dagger a}$. In the Heisenberg picture this transforms the field amplitude operator as $U^\dagger(\theta)aU(\theta) =$

$e^{-i\theta}a$. It thus generates phase shifts. Suppose that θ is a random variable of zero mean and variance σ. Let the rate of the Poisson process be γ. Following the same argument as the damping case we see that the master equation is

$$\dot{\rho} = \gamma \int \mathrm{d}\theta P(\theta)(U(\theta)\rho U^{\dagger}(\theta) - \rho) \qquad (48)$$

where $P(\theta)$ is the probability distribution for θ. Expanding to second order in θ and performing the integration gives

$$\dot{\rho} = \Gamma \mathcal{D}[a^{\dagger}a]\rho \qquad (49)$$

where $\Gamma = \gamma\sigma$. This is the phase diffusion master equation. It is easy to see that it does not cause changes to the mean photon number but the mean amplitude decays at the rate $\Gamma/2$.

The master equation for the laser is not quite as easy to derive. It contains both amplification terms and decay terms but it must also include an effect called saturation. This makes it a non linear amplifier and ensures that it can be stable for any value of the amplifier gain.

In the interaction picture the quantum state ρ of the intracavity laser field at any time satisfies the master equation,

$$\dot{\rho} = Gn_s \mathcal{D}[a^{\dagger}]\left(\mathcal{A}[a^{\dagger}] + n_s\right)^{-1}\rho + \kappa \mathcal{D}[a]\rho \qquad (50)$$

where the super-operators are defined by

$$\mathcal{D}[B]\rho = B\rho B^{\dagger} - \frac{1}{2}(A^{\dagger}A\rho + \rho A^{\dagger}A) \qquad (51)$$

$$\mathcal{A}[B]\rho = \frac{1}{2}(B^{\dagger}B\rho + \rho B^{\dagger}B) \qquad (52)$$

and G is the small signal gain, n_s is the saturation photon number and κ is the cavity decay rate. The inverse superoperator can be represented as

$$\left(\mathcal{A}[a^{\dagger}] + n_s\right)^{-1} = \int_0^{\infty} e^{-\beta(a^{\dagger}a+n_s)/2}\rho e^{-\beta(a^{\dagger}a+n_s)/2} \qquad (53)$$

which describes the incoherent pumping process that leads to saturation of the amplification. The first term in Equation (50) represents gain, that is to say, the injection of energy into the cavity field, while the second term represents photon loss through the cavity mirrors. I have also assumed operation at optical frequencies to ignore thermal photons entering the cavity. Any noise necessarily arises from quantum fluctuations not thermal fluctuations.

The probability, $p_n(t)$, to find n photons in the cavity at time t is given by $p_n(t) = \langle n|\rho(t)|n\rangle$. It then follows from Equation (50) that

$$\frac{\mathrm{d}p_n(t)}{\mathrm{d}t} = Gn_s\left[\frac{n}{n+n_s}p_{n-1} - \frac{n+1}{n+1+n_s}p_n\right]$$
$$+ \kappa(n+1)p_{n+1} - \kappa n p_n \qquad (54)$$

The steady state solution is given by detailed balance [8] as

$$p_n^{ss} = \mathcal{N}\frac{(Gn_s/\kappa)^{n+n_s}}{(n+n_s)!} \qquad (55)$$

where $\mathcal{N}$ is a normalisation constant. Below threshold $G < \kappa$, the steady state distribution may be approximated by

$$p_n^{ss} \approx \frac{1}{1+\bar{n}}\left(\frac{\bar{n}}{\bar{n}+1}\right)^n \qquad G < \kappa \qquad (56)$$

which is analogous to a thermal distribution with

$$\bar{n} = \frac{G}{\kappa - G} \qquad (57)$$

Well above threshold $G \gg \kappa$ the steady state distribution is Poisson with mean

$$\bar{n} = Gn_s/\kappa \qquad (58)$$

This discussion does not make it particularly transparent why we should regard a laser as a clock. Indeed the steady state has no dynamics at all. In order to resolve this we need to study the dynamics of the laser *subject to continuous observation*. This will be an important theme in my discussion of the thermodynamic limits to quantum clocks.

First however I would like to introduce an equivalent classical model. This can be found by computing the dynamics of the average field $\alpha(t) = \mathrm{tr}(a\rho(t))$. Substituting this into the master equation and factorising moments (equivalent to neglecting quantum noise) the semiclassical dynamics is given by

$$\dot{\alpha} = -\frac{\kappa\alpha}{2}\left(1 - \frac{Gn_s}{\kappa(|\alpha|^2 + n_s)}\right) \qquad (59)$$

Well above threshold this is similar to the van der Pol oscillator in a rotating frame. There are two fixed points $\alpha_0 = 0$ and $|\alpha_0|^2 = Gn_s/\kappa$ for $G \gg \kappa$. The second solution is the above threshold limit-cycle solution.

To make a start it is useful to find the stationary two-time correlation function

$$g^{(1)}(\tau) = \frac{\langle a^{\dagger}(t+\tau)a(t)\rangle_{ss}}{\langle a^{\dagger}a\rangle_{ss}} \tag{60}$$

Wiseman shows [16] that, well above threshold, this is given by

$$g^{(1)}(\tau) = e^{-\kappa\tau/4\bar{n}} \tag{61}$$

We can interpret this result as due to quantum phase diffusion noise at the rate $\Gamma = \kappa/2\bar{n}$. Note that this residual phase diffusion occurs at zero temperature unlike the classical case which goes to zero at zero temperature. It suggests an ineliminable source of quantum noise for periodic clocks.

Wiseman [17] presented the theory of a laser subject to continuous heterodyne detection. In the appropriate limit this is a continuous measurement of the real component of the electric field in the cavity in a frame rotating at the cavity frequency. Measurement changes the dynamics of the laser from the standard master equation given in Equation (50). The reason for this is that measurement provides information about the state of the system and thus the conditional state of the system, conditioned on the measurement result must be considered. In other words, quantum state reduction must be modelled explicitly.

To motivate this, suppose that at $t = 0$, the state of the cavity field was projected by some hypothetical fast measurement into a coherent state $|\alpha\rangle$ [18]. This is a state of well defined phase and amplitude. It is clearly not a steady state of the system. How does it subsequently evolve according to Equation (50)? Following Wiseman [17] we can solve the master equation for a short time interval dt in the Fock basis to obtain

$$\rho_{n,m}(\mathrm{d}t) = e^{-|\alpha|^2}\frac{\alpha^n\alpha^{*\,m}}{\sqrt{n!m!}}\left(1 - \frac{\mathrm{d}t(n-m)^2}{2(n+m)}\right) \tag{62}$$

where $\rho_{n,m} = \langle n|\rho|m\rangle$. Well above threshold we can replace $n + m$ in the denominator by $2\bar{n}$. This is the quantum analogue of linearising the noise on the classical limit cycle. It then follows that the short time dynamics is equivalent to that given by the master equation

$$\dot{\rho} = \Gamma\mathcal{D}[a^{\dagger}a]\rho \tag{63}$$

where $\Gamma = \kappa/2\bar{n}$, the well know result for the line width of a laser. Equation (63) is the standard master equation description of phase diffusion. It ensures that the mean photon number does not change while the mean amplitude decays at the rate Γ. This corresponds to a state that is slowly diffusing in phase but all the while remaining of fixed intensity, completely analogous to phase difussion on a limit cycle in the classical case.

In the case of continuous-time measurement we seek an equation that gives the conditional state in an infintesimal time interval dt conditioned on all previous measurement results parameterised by time. This has come to be known as a quantum trajectory [19]. The description has two components: a classical stochastic differential equation to describe the fluctuating classical measurement record and a stochastic master equation to describe the corresponding change in the conditional state at each time step.

In the case of optical heterodyne detection the classical stochastic differential equation describes a photo current record that results when the output of the laser cavity is mixed with a strong coherent local oscillator, detuned from cavity frequency, and then subject to photodetection [19]. This current, suitably normlised, is given by

$$J_{het}(t)\mathrm{d}t = \kappa\langle a(t)\rangle_c\,\mathrm{d}t + \sqrt{\frac{\kappa}{\eta}}\mathrm{d}Z(t) \tag{64}$$

where $0 < \eta \le 1$ is the photo-detector quantum efficiency, $\mathrm{d}Z(t)$ is a complex valued Wiener process and $\langle a(t)\rangle_c$ is the usual trace average computed with respect to the conditional state $\rho_c(t)$ conditioned on the heterodyne current record to time t. This obeys the conditional master equation

$$\mathrm{d}\rho_c = \mathcal{L}\rho_c\,\mathrm{d}t + \sqrt{\frac{\eta}{\kappa}}\mathcal{H}[a]\rho_c\,\mathrm{d}Z^* \tag{65}$$

where the quantum conditioning superoperator $\mathcal{H}[A]$ is defined by

$$\mathcal{H}[A]\rho = A\rho + \rho A - \mathrm{tr}[A\rho + \rho A]\rho \tag{66}$$

and $\mathcal{L}\rho$ is the rest of the master equation given in Equation (50). In essence this superoperator partially 'collapses' the quantum state at each time step. Note that if the system is in a coherent state, for which $a|\alpha\rangle = \alpha|\alpha\rangle$ at any time t, then the noise vanishes as $\mathcal{H}[A]|\alpha\rangle\langle\alpha| = 0$. The conditional master equation tends to localise the conditional states on coherent states. In other words the continuous monitoring of the complex amplitude of the laser field tends to drive the conditional states towards a coherent state.

Well above threshold when operating on the classical limit cycle we may use the phase diffusion master equation in Equation (63) and describe the conditional state of the system by

$$\dot{\rho}_c = \Gamma\mathcal{D}[a^{\dagger}a] + \sqrt{\eta}\mathcal{H}[a]\rho_c\,\mathrm{d}W^* \tag{67}$$

Writing $\rho_c(t)$ as a mixture of coherent states as

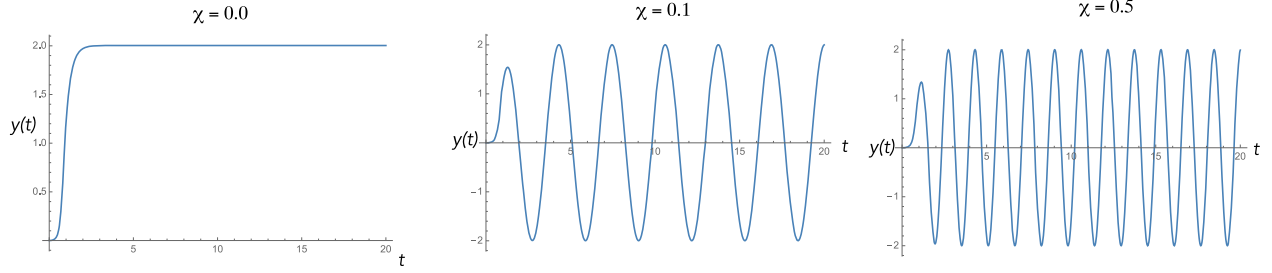$$\rho_c(t) = \int d^2\alpha P_c(\alpha, t)|\alpha\rangle\langle\alpha| \tag{68}$$

Figure 11. Self-pulsing in a laser with an intracavity Kerr non linear medium. The imaginary part of the complex field amplitude for different values of the Kerr non linearity. The parameters are $\epsilon = 0.01, \delta = 0.0, \kappa = 4.0, G = 100, n_s = 1.0$.

and changing variables to $\alpha = re^{i\phi}$ Wiseman[17] shows that in the limit that $\eta \to 1$ the conditional phase dynamics well above threshold when the laser is operating on a limit cycle is stochastic and determined by

$$d\phi_c = \sqrt{\Gamma}\, dW \qquad (69)$$

the standard phase diffusion model seen for a classical limit cycle in the presence of thermal noise. Here however the noise is not thermal in origin but quantum, ultimately due to spontaneous emission from the cavity in this model. The limit-cycle like behaviour emerges only when we consider the conditional state of a laser when the amplitude of the field is continuously monitored.

The frequency of the field on the limit cycle in the original laboratory frame is close to the optical frequency of the cavity. This is very high which makes it impossible to count directly via standard electronic measures. Figuring out ways to do this is the core of atomic clock technology. A first step can be made by including a non linear optical process into the laser cavity. In real optical clocks this is done by using a multi mode treatment to include many longitudinal cavity modes and incorporating an optical non linear process to couple them thus producing a mode locked laser. In the single mode model presented here it suffices to include a single mode optical non linearity such as an atomic absorber or a Kerr non linearity. I will adopt the latter approach.

3.2. Self-modulated laser clocks

A Kerr optical non linearity is a material with an intensity dependent refractive index. In a single mode model this would induce a time dependent detuning that depended on the number of photons in the cavity. With this in mind consider Equation (50) changed to

$$\dot{\rho} = -i\epsilon[a + a^\dagger, \rho] - i\delta[a^\dagger a, \rho] - i\chi[a^{\dagger 2}a^2, \rho]$$
$$+ Gn_s\mathcal{D}[a^\dagger]\left(\mathcal{A}[a^\dagger] + n_s\right)^{-1}\rho + \kappa\mathcal{D}[a]\rho \quad (70)$$

where ϵ is the amplitude of a small noisy injected signal at a carrier frequency δ detuned from the cavity frequency.

The nonlinearity is parameterised by χ in units of frequency. The corresponding semiclassical equation is

$$\dot{\alpha} = -i\epsilon - i(\delta + 2\chi|\alpha|^2)\alpha$$
$$- \frac{\kappa\alpha}{2}\left(1 - \frac{Gn_s}{\kappa(|\alpha|^2 + n_s)}\right) \qquad (71)$$

The inclusion of a small driving term ϵ is important: without it the solutions to the semiclassical equations remain on the unstable fixed point at the origin in the classical limit without noise. It need only be a complex valued Gaussian noise process with zero mean. It is unnecessary to include this in the full quantum model as quantum fluctuations suffice to drive the system. The second term contains the intensity dependent detuning arising from the Kerr non linearity. In Figure 11 I plot some examples of the self-pulsing limit cycle that develops from the original above-threshold laser limit cycle.

A good estimate of the frequency of these oscillations can be found by linearising the dynamics on the limit cycle. Using $\alpha = re^{i\theta}$ we find that the frequency on the limit cycle (for $\delta = 0$) is given by $\Omega = \chi\bar{n}$. The model so far is entirely deterministic and does not include the phase diffusion noise characteristic of a laser operating above threshold. A simple way to do this is to add the required phase diffusion noise for an above threshold laser to the semi classical phase equation to get the Ito equation (with $\delta = 0$)

$$d\theta = -\Omega\, dt + \sqrt{\Gamma}\, dW \qquad (72)$$

where $\Omega = \chi\bar{n}$ and $\Gamma = \kappa/2\bar{n}$. For $\bar{n} >> 1$, the frequency becomes large and the noise becomes small. As previously we define the (dimensionless) energy as $E = r^2$. On the limit cycle the energy is $E_* = \bar{n}$. The rate of change of energy is then given by

$$\dot{E} = -\kappa E + Gn_s = -\kappa E + \kappa\bar{n} \qquad (73)$$

for $G >> \kappa$. The first term represents the rate of energy lost to the cavity via photon emission while the second

term is the rate of energy gain due to the pumping mechanism. The limit cycle forms when these two terms cancel. For a good clock we need the rate of phase diffusion to be small which requires $\bar{n} >> 1$ in which case the energy dissipation is large: a good clock requires a large rate of energy dissipation.

3.3. A quantum nano mechanical clock

In [20] Park et al. demonstrated a nanomechanical oscillator driven by an electron tunnelling current. This system is an example of a periodic clock driven by a quantum noise process as I now show. In the experiment a single C_{60} molecule was bound by van der Waals forces between two gold electrodes. The frequency of the mechanical oscillation was 1.2 THz. The mechanical motion can be approximated by a harmonic oscillator.

Single electrons tunnel on and off the molecule due to a tunnel coupling between a single quasi bound state on the molecule and fermionic reservoirs in the gold electrodes. These reservoirs are biased by a source-drain voltage and thus each is only in local thermodynamic equilibrium with a difference in their chemical potentials determined by the source-drain voltage. The molecule functions as a single electron quantum dot. When an electron tunnels onto the molecule it experiences an electric field that pushes it from the source to the drain whereupon the electron tunnels off the dot into the drain and the van der Waals potential provides a restoring force. In the right regime the molecule shuttles backwards and forwards on a limit cycle between the source and the drain electrode. The nonlinearity responsible for the limit cycle is the exponential dependence of the tunnelling rate on the displacement of the molecule from eqilibrium. A schematic diagram of this is shown in Figure 12.

In [21] a master equation treatment is presented and I will summarise that here. I will assume the so-called 'zero temperature' limit in which, under appropriate bias conditions and very low temperature, the Fermi factor on the left is unity and the Fermi factor on the right is zero. Furthermore I will assume the bias conditions are such that the quasi bound electronic state on the molecule has an energy well below the Fermi level in the source and well above the Fermi level in the drain. This ensures that low temperature fluctuations in the occupation close to the Fermi levels are not important.

When electrons tunnel out of the source and onto the drain the external circuit increments/decrements the charge in the source/drain to ensure that they each remain in local thermodynamic equilibrium, i.e. keep a constant chemical potential. This links fundamental quantum discrete tunnelling events to fluctuations of the current and voltages in the external circuit.
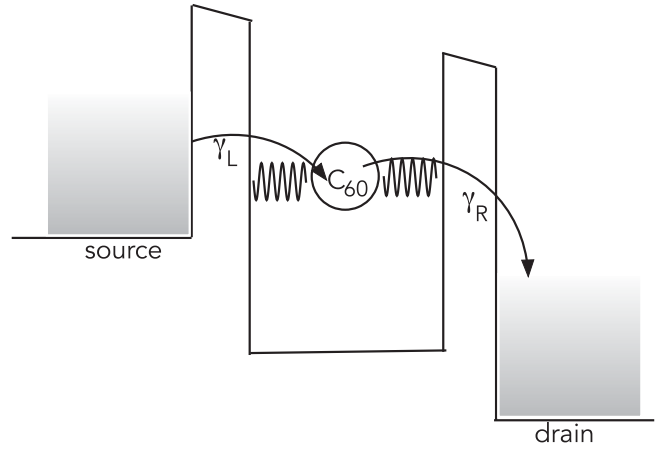

Figure 12. A schematic representation of a single harmonically bound quantum dot between two electrodes. Electrons tunnel onto the dot from the left and off the dot to the right. The bare tunnelling rates $]\gamma_L, \gamma_R$ are exponentially modulated by the displacement of the dot from equilibrium.

The dynamical variables are the mean number of electrons on the molecule $\bar{n}$ and the mean displacement X and mean conjugate momentum Y of the oscillator. The semiclasscial equations are obtained by calculating the equations of motion for these first order moments, using the master equation, and factorising all higher order moments;

$$\frac{d\bar{n}}{dt} = \gamma_L(1 - \bar{n})e^{-4\eta X} - \gamma_R \bar{n} e^{4\eta X} \qquad (74)$$

$$\frac{d\alpha}{dt} = -i\nu\alpha - \frac{\kappa}{2}\alpha + i\chi\bar{n} \qquad (75)$$

with

$$\alpha = \langle a \rangle = \langle \hat{x} \rangle/(2\lambda\eta) + i\langle \hat{p} \rangle \lambda\eta/\hbar \equiv X + iY.$$

with ν the mechanical frequency of the molecular motion and

$$\chi = eE\eta\lambda/\hbar \qquad (76)$$

$$\eta = \left(\frac{\hbar}{2m\nu}\right)^{1/2}\frac{1}{\lambda} \qquad (77)$$

while λ sets the scale for the spatial dependence of the tunnelling rates on the molecular displacement from equilibrium, e is the electronic charge and E is the applied static electric field across the source-drain junction and κ is the rate of energy dissipation in the mechanical oscillator. The system of equations, Equation (74), (75) has a fixed point, which undergoes a Hopf bifurcation with increasing χ to a limit cycle forming the clock. The details can be found in [21]. Note the similarity between these equations and the equations of motion for the quartz oscillator coupled to a Schmidtt trigger given
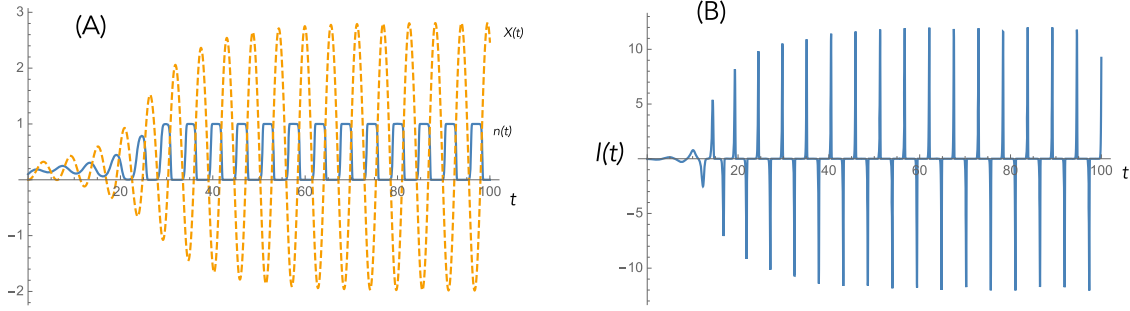
Figure 13. A typical limit cycle for the semiclassical model of a nanomechanical resonator coupled to tunnel junctions. (a) The charge, $n(t)$ and $x(t) = Re(\alpha(t))$ are plotted versus time. (b) The corresponding average current through the system, $2I(T)/e$. Parameters are $\gamma_L = \gamma_R = 0.1, \nu = 1.0, \eta = 1.0, \chi = 1.0, \kappa = 0.1$.

in Equation (38) with $g(V) = 2V - 1$. A typical limit cycle is shown in Figure 13.

A statistical description of the semiclassical dynamics can also be obtained from the master equation. The telegraph signal is determined by two point processes $dN_L(t)$ and $dN_R(t)$. When an electron tunnels onto the molecule in a time dt, $dN_L(t) = 1$. Like wise when an electron on the molecule tunnels off in a time dt, $dN_R(t) = 1$. The master equation determines the average values of these point processes in terms of quantum averages;

$$E[dN_L(t)] = \gamma_L \langle e^{-4\eta\hat{X}}(\hat{n} - 1)\rangle \, dt \qquad (78)$$

$$E[dN_R(t)] = \gamma_R \langle e^{4\eta\hat{X}}\hat{n}\rangle \, dt \qquad (79)$$

where $\hat{X}$ is the displacement operator for the mechanical motion and $\hat{n}$ is the number operator for the number of excess electrons on the molecule. Correlations (entanglement) between the electronic and motional states means these moments do not factorise in general. The conditions for which factorisation is a good approximation (see [21]) define the semiclassical approximation. In that case the two Poisson processes become inhomogeneous point processes and the occupation probabilities obey

$$\dot{p}_1(t) = \gamma_L p_0(t) e^{-4\eta X(t)} - \gamma_R p_1(t) e^{4\eta X(t)} \qquad (80)$$

The important point is that, unlike the apparently similar Quartz model Equation (38), the noise in this case is not thermal diffusion in momentum but rather intrinsic quantum fluctuations arising from single electron tunnelling events. Nonetheless I will show that the limit for a good clock requires a large amount of energy dissipation.

What is the clock signal? To answer that question we need to understand how the fundamental quantum tunnelling events are related to the current in the external circuit. These tunnelling events define conditional Poisson stochastic process $dN_L(T)$ and $dN_R(t)$ for left and right tunnelling events that take the values 0, 1 in an increment of time dt, where 1 corresponds to a single

tunnelling event. The rates for these process are conditioned by quantum averages. In a completely symmetric tunnelling scheme, $\gamma_L = \gamma_R = \gamma$, the average current is given by the classical stochastic process

$$I(t) \, dt = \frac{e}{2}(dN_L(t) + dN_R(t)) \qquad (81)$$

It follows that in the semiclassical limit the average current is given by

$$\bar{I}(t) = \frac{e\gamma}{2}\left(e^{-4\eta X}(n - 1) + e^{4\eta X}n\right) \qquad (82)$$

An example is given in Figure 13.

The quantum dynamics is given by solving the master equation given in [21]. If no attempt is made to monitor the current, the dynamics is given by the unconditional master equation. A typical example is shown in Figure 14.

On the other hand if tunelling events are monitored using the current through the molecule, the dynamics is given by a conditional master equation. A typical example is shown in Figure 15. The fluctuations in the clock period arising from the stochastic nature of quantum tunnelling events is now evident. This leads to phase and amplitude fluctuations in the dynamics of the mechanical oscillations limiting the accuracy of the clock.

On the limit cycle we define $X(t) = r_* \sin(\Omega t)$, $Y(t) = r_* \cos(\Omega t)$ where r_* is the amplitude of the limit cycle and
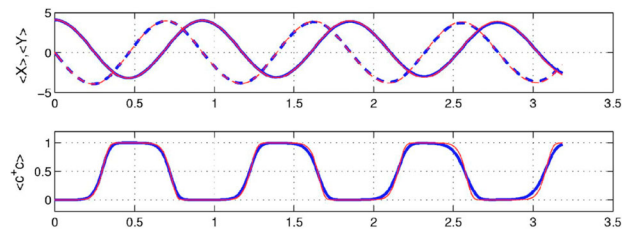

Figure 14. The unconditional quantum dynamics of the nanomechanical oscillator in terms of the quantum averages $\langle c^\dagger c\rangle$, and average displacement and momentum, $\langle X\rangle$, $\langle Y\rangle$. Parameters are $\gamma_L = \gamma_R = 1.0, \nu = 1.0, \eta = 0.3, \chi = '1.0, \kappa = 0.05$ reproduced with permission from [21].
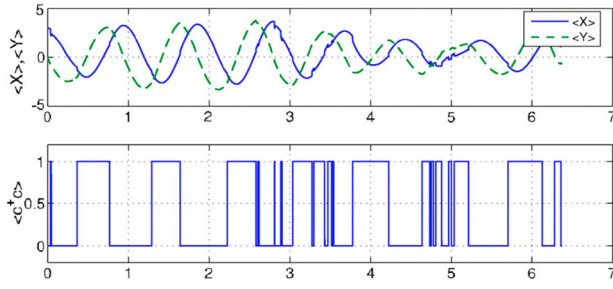
Figure 15. Typical conditional quantum dynamics of the nanomechanical oscillator in terms of the conditional quantum averages $\langle c^\dagger c \rangle$, and average displacement and momentum, $\langle X \rangle$, $\langle Y \rangle$. Parameters are $\gamma_L = \gamma_R = 1.0, \nu = 1.0, \eta = 0.3, \chi = 1.0, \kappa = 0.05$ reproduced with permission from [21].

Ω is the frequency. Using the same two-time averaging procedure that I used in Section 2.2, to a good approximation r_* is given by the solution to the transcendental equation

$$e^{\mu x^2} = \cosh x \qquad (83)$$

where $x = \eta r_*$ and $\mu = \kappa \pi / (4 \eta \chi)$. The frequency is well approximated by ν with small corrections of order ν^{-2}.

On the limit cycle the two inhomogeneous point processes describing the tunnelling events in the semiclassical limit are determined by the intensity functions

$$\lambda_L(t) = \gamma e^{-4\eta r_* \sin(\Omega t)} \qquad (84)$$

$$\lambda_R(t) = \gamma e^{4\eta r_* \sin(\Omega t)} \qquad (85)$$

The waiting time probability function for an electron to tunnell off the molecule is then given by

$$Pr(n(t) = 1 | n(0) = 1) = \exp\left[-\int_0^t dt' \lambda_R(t') \right] \qquad (86)$$

The regularity of the clock can be seen in the time derivative of the integrated count $N_R(t)$ for the process $dN_R(t)$. This is shown in Figure 16 for various values of r_*. In (A) the pure Poisson process with rate γ is shown. This corresponds to $r_* = 0$. As the size of the limit cycle increases the process becomes more regular. Similar results hold for $Pr(n(t) = 0 | n(0) = 0)$. This means that in the limit of large limit cycles, the period of the conditional motion becomes increasingly regular and a good clock results.

The thermodynamic constraints on this system are similar to the quartz clock with the important exception that here fluctuations are due entirely to quantum tunnelling not thermal effects. As before the size of the limit cycle determines both the average energy dissipated and the quality of the clock. The semiclassical equations imply that the rate of change of the energy of the oscillator (in dimensionless units), $E = (X^2 + Y^2)/2$ is

$$\dot{E} = -\kappa E(t) + \chi Y(t) n(t) \qquad (87)$$

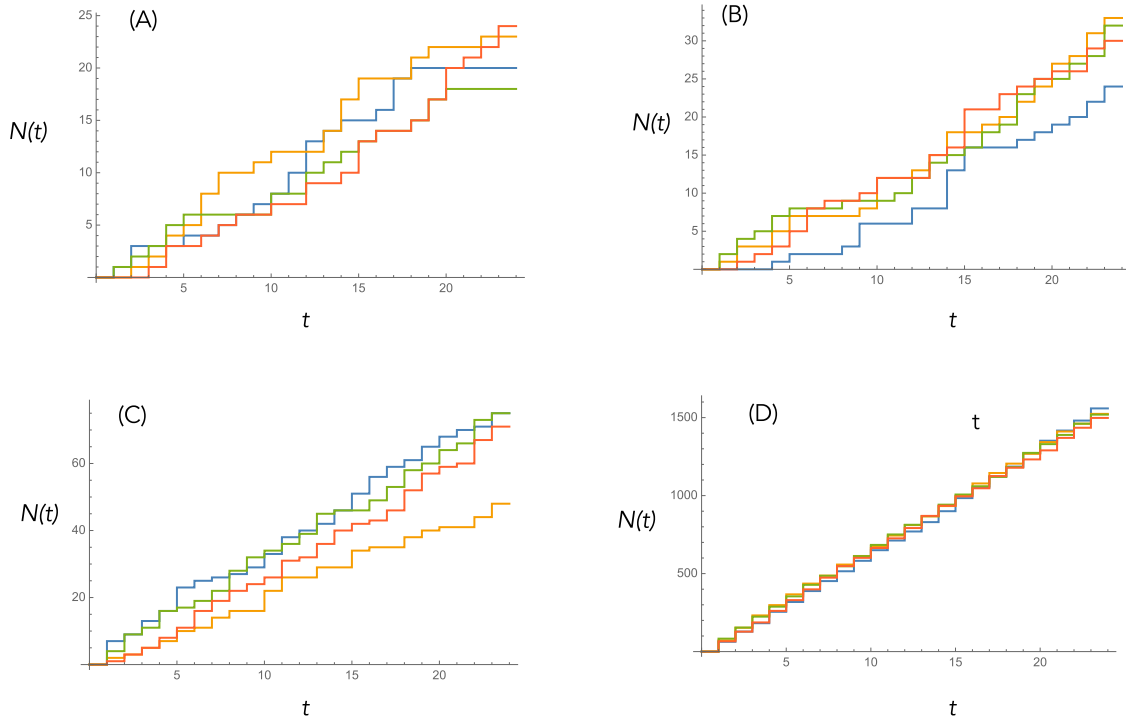The first term on the right is energy lost due to damping into mechanical environment, this time at (near) zero

Figure 16. A simulation of integrated count $N_R(t)$ for the process $dN_R(t)$, given that the molecule is occupied at $t = 0$, for increasing values of the amplitude of the limit cycle r_*, (a)$r_* = 0$, (b)$r_* = 1.0$, (c)$r_* = 2.0$, (d)$r_* = 5.0$ and $\gamma_L = \gamma_R = 1.0, \Omega = 2\pi, \eta = 0.3$.

temperature, while the second term is the electrical work done by the electrical field when the dot is occupied. The argument runs through in a similar fashion to the case in Section 2.2. In the limit of large limit cycle amplitude, r_* large, the work done over one cycle, starting at the time $(n(0) = 1)$, is given by the integral of $Y(t)$ over a single cycle which ends when the electron tunnels off the molecule at a time $t_\downarrow \Omega = \pi$ The work done on the k'th cycle is just the integral

$$W_k = \chi r_* \int_0^{t_\downarrow} dt \, \sin(\Omega t) = \frac{2\chi r_* T_k}{\pi} \qquad (88)$$

where $T_k = t_\downarrow$ and r_* is the radius of the limit cycle. Again this is in dimensionless units; to convert to SI units, multiply by $\hbar v$. As the work done on this cycle equals the energy lost due to damping Q_k we find that

$$Q_k = \frac{2\chi r_* T_k}{\pi \kappa} \qquad (89)$$

On average the energy dissipated depends on the average time the single electron occupies the molecule. Thus over a long time τ, the average energy dissipated is determined by the average fraction of time the dot is occupied. Using standard results for a random telegraph signal we see that

$$\bar{Q} = \frac{2\chi r_* \tau}{\pi \kappa} \left(\frac{\gamma_L}{\gamma_L + \gamma_R} \right) \qquad (90)$$

This quantity is dimensionless (to convert to SI units multiply by $\hbar v$). This example shows that, even at zero temperature, quantum fluctuations ensure that a good clock requires a large limit cycle r_* and this corresponds to large energy dissipation in the molecular motion.

There is one final thermodynamic lesson to take away from this example. The system is ultimately driven by the different chemical potentials in the Fermi reservoirs in the source and drain. The average energy that must be dissipated in the external circuit is given by $eV_{SD}(\mu_L - \mu_R)$ where e is the electronic charge, V_{SD} is the source drain bias voltage and $\mu_{L/R}$ are the chemical potentials in the left and right reservoirs. That the chemical potentials are the not the same of course indicates that the entire system is not in thermal equilibrium; the essential requirement for a clock to operate. The free energy has been increased by electrical work done on it by the external circuit. Erker et al. [11] give an interesting example in which a clock is driven by a difference in temperature (the other Lagrange multiplier) between two reservoirs. There is another very important class of clock that is driven by a difference in chemical potential; the chemical clocks that characterise biological systems. Perceived time is determined by the irreversible processes in such clocks [22].

4. Non periodic clocks: information as fuel

At first sight the notion of a non periodic, irreversible clock seems paradoxical: a clock is the very epitome of a deterministic periodic system. Yet irreversible clocks have long been used, water clocks for example, and a particular irreversible clock is in common usage. Radio-carbon dating is based on the stochastic and irreversible decay of a radionuclide – C^{14}. Metabolism ensures living organisms will continually refresh their concentration of C^{14} while alive, but once dead the concentration begins to relax to the steady state non-organic concentration of C^{14} in the environment. Indeed, in radiocarbon dating one must take into account that different organisms die with differing concentrations of C^{14}. Furthermore, the vital concentration may change with time due to concentration of C^{14} in the atmosphere changing over time. In other words, different organisms and different epochs do not necessarily begin with the same non equilibrium distribution. As we will see, relaxation from a non equilibrium state is a key feature of non deterministic clocks, especially when the non equilibrium state is a result of state conditioning of a system subject to measurement.

4.1. Radio carbon clock

It is known that the probability of a single radionuclide not to decay in a time t is $\exp(-\gamma t)$, where γ is called the decay rate. Given an ensemble of undecayed radionuclides, the number that have decayed after some time t is a Poisson distributed stochastic variable N with mean γt. Thus, given a count of the number of radionuclides that have decayed, N, we may estimate the time that has elapsed as

$$t_{\text{est.}} = \frac{N}{\gamma}. \qquad (91)$$

The error in this estimate is given by the fluctuations in the final count δN for a fixed estimate $t_{\text{est.}}$. Since for a Poisson process the variance is equal to the mean, one finds the relative error is

$$\frac{\delta t_{\text{est.}}}{t_{\text{est.}}} = \frac{1}{\sqrt{\gamma t_{\text{est.}}}}. \qquad (92)$$

Conveniently, we get a better estimate the longer we wait. Now, in the case of radio-carbon dating, one indeed wishes to compute the elapsed time $t_{\text{est.}}$, and so one requires to know γ before hand; calibrate the clock. However, conversely, one could instead take this system as defining a temporal scale, where to take the time would be to make the count N, and the value of γ would merely reflect a particular choice of units and thus be purely conventional. That is, the actual count N, while subject to fluctuations, is a local physical quantity that can serve as
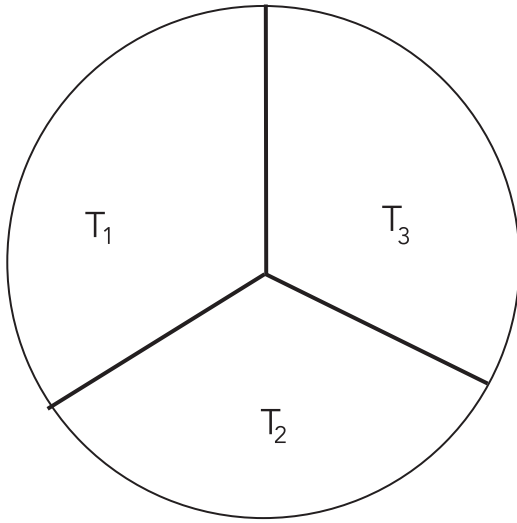
Figure 17. A schematic diagram of Mach's hypothetical thermal clock. Three identical materials, initially at different temperatures, are placed in thermal contact but completely isolated from the rest of the universe. By monitoring the temperature of any one of them, elapsed time can be estimated.

physical time. Yet it is worth noting that a radionuclide can only decay, i.e. N can only increase, so in contrast to the prototypical reversible clock, this is a clock with no tock.

4.2. Mach's thermal clock

Mach's thermal clock was an attempt to ground an understanding of time in our sense perception of irreversible processes [23]. Mach's clock is a thermodynamic system in which three identical materials, initially held at different temperatures, are placed in thermal contact but thermally isolated from the rest of the universe, see Figure 17.

As the system is isolated, the internal energy, U cannot change with time, thus

$$\dot{U} = c(\dot{T}_1 + \dot{T}_2 + \dot{T}_3) = 0 \qquad (93)$$

where c is the specific heat. Thus $T_1(t) + T_2(t) + T_3(t) = T_1(0) + T_2(0) + T_3(0)$, a constant. Newton's law of cooling, is an empirical law that says the rate of change of temperature is proportional to the temperature difference. It is used by forensic pathologists. In this case it implies that

$$\dot{T}_1 = k(T_3 - T_1) + k(T_2 - T_1) \qquad (94)$$

which is clearly negative and k is a constant. Using similar relations for the other temperatures we find that

$$\bar{T} - T_1(\tau) = Ae^{-3k\tau} \qquad (95)$$

where $A = \bar{T} - T_1(0)$ is a constant and we have defined the initial average temperature as $\bar{T} = (T_1(0) + T_2(0) + T_3(0))/3$. This is very like radioactive decay. Given a good thermometer, it is possible to estimate the time and conversely. Equation (95) implies that the uncertainties satisfy

$$\frac{\Delta T_1}{T_1} + \frac{\Delta \tau}{\tau_{est}} = 0 \qquad (96)$$

where I have defined an estimated time by $\tau_{est} = 1/3k$ in analogy with radioactive decay.

4.3. A classical thermal oscillator clock

A simple harmonic oscillator in thermal equilibrium with a bath at temperature T is in a stable stationary state. This would seem an unlikely place to start from to make a clock yet it can be done if we allow accurate measurements. The reason is simple: if the state of the system is conditioned on the result of an accurate measurement (of displacement say) it is no longer in thermal equilibrium and can exhibit time dependent features if the measurement is continuous in time. In effect the measurement lowers the entropy of the system thereby increasing its free energy and taking it out of equilibrium. In this case it is information gain by the measurement apparatus that raises the free energy of the system not work provided by a battery. This system does not have a limit cycle; it is driven entirely by thermal fluctuations.

In what follows I will assume that the measurements are perfectly accurate so that we can track individual stochastic trajectories of an oscillator in phase space. In that case the dynamics is given by the Ito stochastic differential equations in Equation (13), As in the case of the pendulum clock we now change to polar coordinates for amplitude and phase $x(t) = r(t)\cos(\phi(t))$, $y(t) = r(t)\sin(\phi(t))$.

$$dr(t) = -\Gamma r(t)\, dt + \frac{\sigma^2}{2r}\, dt + \sigma\, dW_r(t) \qquad (97)$$

$$d\phi(t) = -\omega\, dt + \frac{\sigma}{r}\, dW_\phi(t) \qquad (98)$$

with dW_r, dW_ϕ independent Wiener processes and time is measured in units of the oscillator period. Clearly both phase and amplitude fluctuate.

The energy is defined as $E = r^2/2$ so

$$\frac{d\bar{E}}{dt} = -2\Gamma E + \frac{D}{2} \qquad (99)$$

In long time limit the energy is $\bar{E} \to \frac{\sigma^2}{4\Gamma}$ an illustration of the fluctuation-dissipation theorem. Now define
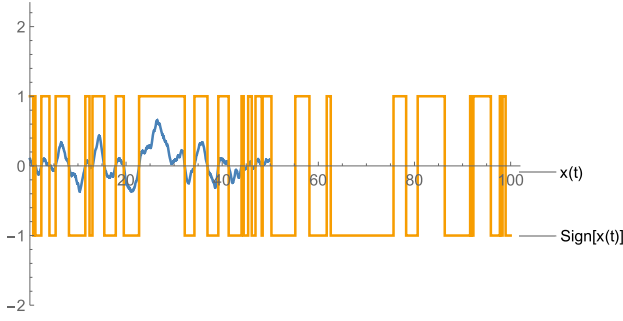
Figure 18. A sample path for $x(t)$ and a processed sample path $s(t) = \text{sign}(x(t))$. $Q = 0.5$.
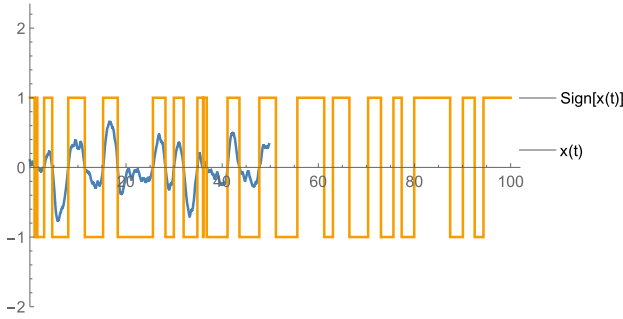

Figure 19. A sample path for $x(t)$ and a processed sample path $s(t) = \text{sign}(x(t))$. $Q = 1$.

a dimensionless time $\tau = \omega t$ and set $r \to \bar{r} = \sqrt{2\bar{E}} = \sqrt{\frac{D}{2\Gamma}}$. The phase diffusion rate is

$$d\phi(\tau) = -d\tau + \sqrt{\frac{2}{Q}} \, dW_\phi(t) \qquad (100)$$

where $Q = \omega/\gamma$, the quality factor. Clearly a high quality factor, Q is needed for a well defined frequency. To increase the resolution the frequency is increased with Q held constant for a given accuracy. This necessarily increases the rate of energy dissipation.

In Figures 18–20 I plot a sample path for $x(t)$ and a processed sample path $s(t)$ for increasing oscillator quality factors Q. The processing simply takes the signal $x(t)$ and computes $s(t) = \text{sign}[x(t)]$. This makes it particularly easy to separate phase and amplitude fluctuations and to estimate fluctuations in the clock period. The increasing accuracy of the clock with increasing Q is evident.

This kind of clock has been demonstrated by the Pearson et al. [24] using a cold nanomechanical membrane and an optomechanical circuit transducer that enabled a very accurate measurement of the displacement of the oscillator. The experiment confirmed the thermodynamic trade off between resolution/accuracy and heat dissipated. Good clocks generate a lot of entropy.
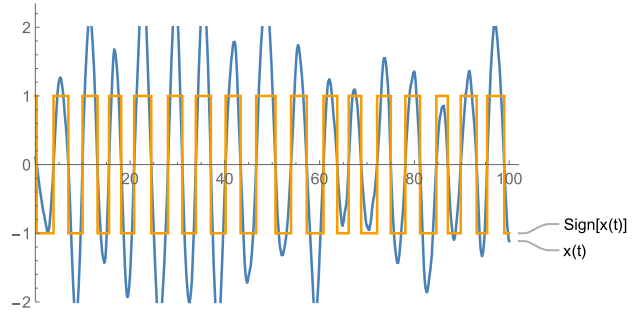

Figure 20. A sample path for $x(t)$ and a processed sample path $s(t) = \text{sign}(x(t))$. $Q = 10.0$.

4.4. Quantum thermal clocks

A simple generalisation that introduces temperature in a fundamental way results if we consider a two-level system (TLS) in a thermal bath at temperature T (radiative damping). While the ensemble average is a stationary state in equilibrium with the bath, continuous measurement of the energy of a single realisation (discussed in more detail below) yields a random telegraph signal. Let us define the random telegraph signal $Z(t)$ to take the value $Z(t) = -1$ if the two-level system is found in the ground state $|g\rangle$ and $Z(t) = 1$ if it is found in the excited state $|e\rangle$. The conditional state at time t, given the measurement record up to that time, is then

$$\rho_{\text{cond.}}(t) = \frac{1 + Z(t)}{2}|e\rangle\langle e| + \frac{1 - Z(t)}{2}|g\rangle\langle g|. \qquad (101)$$

On the other hand, the ensemble average – the average over all possible random telegraph signals – yields the thermal state

$$\rho_{\text{th.}}(\beta) = \frac{1 - \tanh(\beta\epsilon/2)}{2}|e\rangle\langle e| + \frac{1 + \tanh(\beta\epsilon/2)}{2}|g\rangle\langle g| \qquad (102)$$

where $\beta = 1/k_B T$ with T the temperature of the bath, k_B is Boltzmann's constant and ϵ is the energy separation between $|g\rangle$ and $|e\rangle$. (The convention is $|g\rangle$ is assigned energy $-\epsilon/2$ and $|e\rangle$ is assigned energy $\epsilon/2$.) The transition rate from $|e\rangle$ to $|g\rangle$ is $\gamma(\bar{n}+1)$ and that from $|g\rangle$ to $|e\rangle$ is $\gamma\bar{n}$ where $\bar{n} = [\exp(\beta\epsilon) - 1]^{-1}$ is the bath occupation and γ is the spontaneous emission rate. At temperatures and energies such that $\bar{n} \gg 1$ we can neglect spontaneous emission and these rates are the same.

A simple irreversible clock can now be defined operationally by counting the number of transitions N. As before, N is a Poisson distributed stochastic variable, but this time with parameter $\gamma\bar{n}$, which depends on temperature. In the high-temperature limit, the equivalent to

Equation (91) reads

$$t_{\text{est.}} = \frac{N}{\gamma \bar{n}} \approx \frac{\epsilon N}{\gamma k_B T}. \qquad (103)$$

The error in the estimate scales as $(\gamma \bar{n})^{-1/2}$. As is the case for periodic clocks, the greater the rate of energy dissipated the better the clock. This is the key result of Erker et al. [11].

In contrast to the example from radiocarbon dating, here the relative error in $t_{\text{est.}}$ is limited by the relative error in the temperature, T. That is, in order for this system to define an accurate temporal scale, we require a good thermometer. Conversely, we may use this system as a thermometer where the temperature is estimated from elapsed time,

$$k_B T_{\text{est.}} = \frac{\epsilon N}{\gamma t}, \qquad (104)$$

so one may equally well say that in order for this system to define an accurate temperature scale, we require a good clock. For a fixed count N, and a given two-level system, we see that for high temperature,

$$t_{est}.T_{est} = constant \qquad (105)$$

which implies that

$$\frac{\delta t_{\text{est.}}}{t_{\text{est.}}} + \frac{\delta T_{\text{est.}}}{T_{\text{est.}}} = 0. \qquad (106)$$

This is the same structure that was derived for the Mach clock in Equation (96) and suggests a special relationship between time and temperature that I will return to in section Sections 5.1, 5.2. An elegant treatment of the statistical connection between time and temperature has recently been given by Tanaka [25] using the Fisher information metric associated with estimation of time and temperature.

There is a hidden assumption in this treatment: I have assumed that one can indeed monitor the state of a single TLS and thus accurately sample the random telegraph process $Z(t)$. In this assumption I have in effect smuggled in a very low entropy bath to ensure the measurements do indeed provide reliable information on the state of the TLS. In this type of clock, the conditional state of the system is pushed away from thermal equilibrium, and the free energy raised, not by doing work but by extracting entropy through good measurements. In this sense, information is fuel.

4.5. A superconducting quantum thermal clock

It is not easy to make detectors that count individual quantum jumps of a quantum system but it is a standard measurement for a TLS based on superconducting
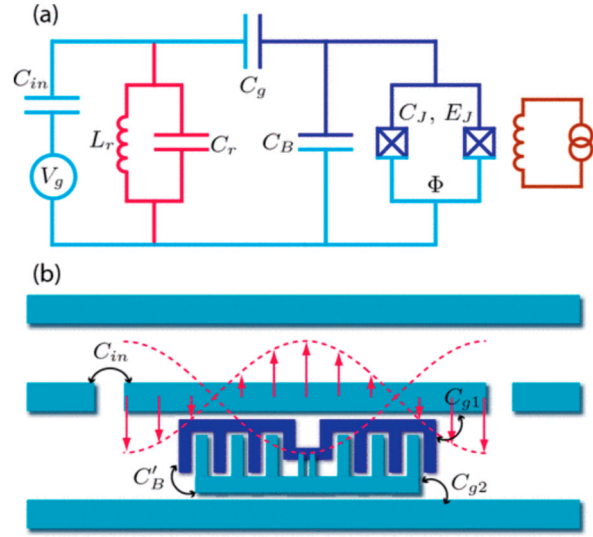

Figure 21. An equivalent circuit model for a superconducting transmon in a co planar cavity together with a schematic representation of the device. Reproduced with permission from Koch et al Phys. Rev. A 76, 042319 [27].

quantum circuits [26]. These are devices based on the Josephson effect in superconductors at very low temperatures. A typical such device is known as a transmon [27] depicted in a highly simplified schematic form in Figure 21.

A small metal superconducting island is separated from a reservoir of Cooper pairs by tunnelling junctions. Cooper pairs can tunnel on and off the island though the Josephson effect. Furthermore a hole is introduced into the junction forming a 'split junction'. By changing the magnetic flux through this hole, the coupling energy between the transmon and the reservoir can be changed, effectively changing the rate of the tunnelling. In addition, the island can be capacitively coupled to a neighbouring superconducting bias line enabling the Coulomb energy of the transmon to be changed. Thus there are two 'handles' for changing the energy of the transmon. By carefully adjusting the ratio of the capacitive coupling to the tunnel coupling a discrete energy spectrum results. These levels are not equally spaced enabling a microwave voltage source on the capacitive coupling to be resonant only with transitions from the ground state to the first excited state. This is the two-level system of interest. The microwave voltage is sustained in driven superconducting cavity containing the transmon. Effectively this constitutes a simple TLS in an electromagnetic cavity that may be thermally or coherently driven, or both.

We now require a way to measure the state of the TLS. This is based on the method of dispersive coupling [28]. The transmon can be simultaneously coupled

to a second cavity with a resonant frequency that is well-detuned from the TLS transition frequency. In this case transitions between the energy eigenstates of the TLS are suppressed but the cavity frequency can be shifted by different amounts depending on the state of the TLS. This is a non linear dispersion. Reciprocally, the energy difference between the states of the TLS are shifted by an amount proportional to the intensity of the field in the cavity. In atomic physics this is known as the dynamic Stark effect. We will refer to this dispersively coupled cavity as the *readout cavity*. For a more detailed discussion see Section 3.10.2 of [19]

If the readout cavity is thermally isolated and coherently (but weakly) driven, the steady state field inside the cavity is in a coherent state: a pure state of zero entropy. The amplitude of this state depends on the detuning of the driving field from the readout cavity resonance frequency. But as this resonance frequency is shifted by the TLS, the phase of the field emerging from the cavity will change depending on the state of the TLS. If this phase is continuously monitored using homodyne detection, a continuous measurement record of the changing state of the TLS can be inferred under the right conditions. One of these conditions is that the readout cavity must be subject to very little thermal excitation so that it remains close to a coherent state. This amounts to assuming that the readout system has very low entropy thus making explicit the necessity for another very low temperature heat bath for the thermal clock to function.

To implement a thermal clock with this system, the TLS must be coupled to a thermal radiation field. This can be simulated by driving the TLS with an additional Gaussian noise field at the TLS resonance to implement controllable thermal noise acting on the transmon. A schematic of this temperature clock is given in Figure 22.
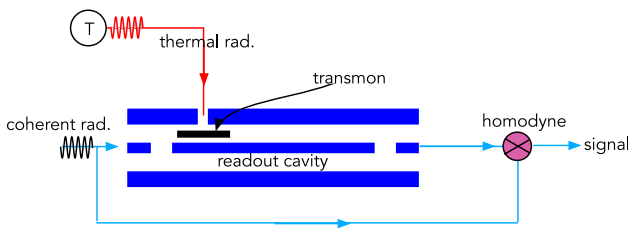

Figure 22. A quantum superconducting thermal clock. A transmon two-level system (TLS) is dispersively coupled to a coplanar waveguide cavity on a chip. A coherent microwave field is transmitted through the cavity and detected via homodyne mixing producing a signal that monitors the state of the TLS in real time. To produce a non periodic thermal clock the TLS is driven by high-temperature (T) noise, generated by an arbitrary wave generator and up-converted to the TLS frequency with the help of an external microwave source [Figure courtesy of Arkady Fedorov].

The joint quantum state of the resonator and the readout qubit satisfies the master equation

$$\dot{\rho} = -iE[a + a^\dagger, \rho] - i\chi[a^\dagger a \sigma_z, \rho]$$
$$+ \gamma(\bar{N} + 1)\mathcal{D}[\sigma_-]\rho + \gamma\bar{N}\mathcal{D}[\sigma_+]\rho + \kappa\mathcal{D}[a]\rho,$$

where E is the amplitude of the coherent driving field driving the measurement cavity, χ is the strength of the dispersive coupling between TLS and cavity, κ, γ are the energy decay rates of the readout cavity and TLS respectively, and $\bar{N}$ is the mean excitation in thermal radiation coupled to the TLS. The final four terms describe irreversible evolution. The superoperator appearing in these terms is defined, as previously, by $\mathcal{D}[A]\rho = A\rho A^\dagger - \frac{1}{2}A^\dagger A\rho - \frac{1}{2}\rho A^\dagger A$.

Note that the coupling of the TLS to the cavity is proportional to the energy of the TLS which ensures that this coupling, of itself, cannot change the energy distribution of the TLS but it does change the detuning of the measurement cavity, conditional on the state of the TLS, and thus changes the amplitude of the field emitted. The homodyne current (scaled by γ) of the emitted field is given by

$$I(t) = \langle a + a^\dagger \rangle_c + \xi(t)/\sqrt{\gamma\eta} \tag{107}$$

where $\xi(t)$ is a white noise process, $0 < \eta < 1$ is the homodyne detection efficiency, γ is the TLS energy decay rate. This classical stochastic process will be used to monitor the quantum jumps of the TLS and thus constitutes the counter for the thermal clock.

While the current $I(t)$ is a classical stochastic process it's statistics is conditioned on the quantum source; thus the subscript on the quantum average in the first term. The conditional state, conditioned on a particular current history can be computed using the method of quantum trajectories [19]. In effect this describes a continuous stochastic state reduction up to time t. This state obeys the stochastic master Equation [19]

$$d\rho_c = -iE[a + a^\dagger, \rho_c] - i\chi[a^\dagger a \sigma_z, \rho_c]$$
$$+ \gamma(\bar{N} + 1)\mathcal{D}[\sigma_-]\rho_c + \gamma\bar{N}\mathcal{D}[\sigma_+]\rho_c$$
$$+ \kappa\mathcal{D}[a]\rho_c + \sqrt{\kappa\eta}\mathcal{H}[a]\rho_c\, dW(t),$$

where $dW(t)$ is a classical Wiener process and $\mathcal{H}[A]\rho = A\rho + \rho A^\dagger - \text{tr}(A\rho + \rho A^\dagger)$.

To operate as a pure entropy clock, it is necessary to distinguish quantum jumps in the TLS due to thermal excitations. To this end we will assume that the readout cavity is strongly driven and rapidly damped. In this limit the state of the TLS obeys the effective master equation in

the Schrödinger picture,

$$\dot{\rho} = -i(\Delta + \epsilon/\hbar)[\sigma_z, \rho] + \gamma(\bar{N} + 1)\mathcal{D}[\sigma_-]\rho$$

$$+ \gamma\bar{N}\mathcal{D}[\sigma_-]\rho + \Gamma\mathcal{D}[\sigma_z]\rho, \qquad (108)$$

where $\Delta = 4\chi E^2/\kappa^2$ and $\Gamma = 4\Delta\chi/\kappa$. The last term in the master equation leads to pure phase-diffusion around the z-axis on the Bloch sphere and decay of the TLS polarisation but cannot change the steady-state of the TLS which remains thermal. It also describes a continuous measurement of σ_z as I now explain.

The observed record is the homodyne stochastic photocurrent exiting the readout cavity of the qubit that now becomes

$$I(t)\,dt = \langle\sigma_z\rangle_c\,dt + dW(t)/\sqrt{\eta\Gamma}, \qquad (109)$$

The conditional stochastic master equation now takes the form

$$d\rho_c = -i(\Delta + \epsilon/\hbar)[\sigma_z, \rho_c]\,dt + \gamma(\bar{N} + 1)\mathcal{D}[\sigma_-]\rho_c\,dt$$

$$+ \gamma\bar{N}\mathcal{D}[\sigma_+]\rho_c\,dt + \Gamma\mathcal{D}[\sigma_z]\rho_c\,dt$$

$$+ \sqrt{\eta\Gamma}\mathcal{H}[\sigma_z]\rho_c\,dW(t)$$

The condition to see quantum jumps is $\Gamma >> \gamma\bar{N}$ which ensures that information about the energy of the TLS is acquired faster than it is changed by thermal transitions. In Figure 23 I plot the conditional mean of σ_z showing quantum jumps. In this limit the system is operating as a thermal clock driven by reductions in entropy due to the measurement. In other words, when the rate of information gain by an observer exceeds the rate of thermally driven fluctuations we obtain a thermal clock. In this limit the free energy of the clock is increased by entropy
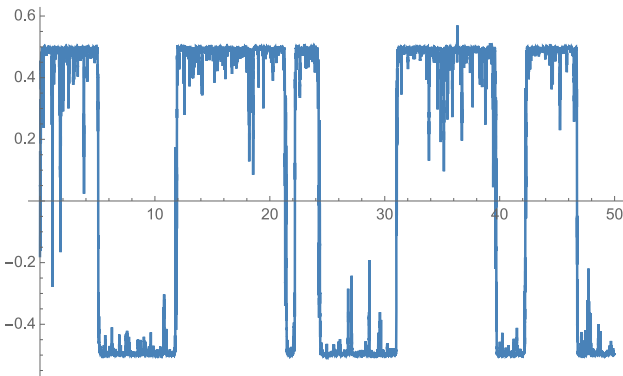

Figure 23. The conditional mean energy of the TLS (in units of ϵ) versus time in the good measurement limit. The jumps are caused by photons entering and exciting the TLS from the thermal bath coupled to it. The mean thermal photon number in the bath was $\bar{N} = 0.9$ and $\Gamma = 5.0$, $\gamma = 0.1$.

reduction rather than work done as in the typical periodic clock.

4.6. A thermal superradiant clock

There are many engines driven by the transfer of heat from a hot to a cold bath [29]. An interesting model of clock driven in this way is given by Erker et al. [11]. I will now describe a physical implementation of a similar model using a superradiant ensemble of two-level systems. In that model, the idea is to use a temperature difference between two qubit reservoirs to excite another multi-level system which then emits a photon. The multi-level system is like a battery which is charged up by a heat current. When it is fully charged it emits a photon. I will replace the two qubits with two optical cavities and change the battery to a super radiant atomic ensemble. This changes the nature of emission from the battery system to a spontaneous emission model.

It is not possible for thermal excitations to pass from one system in thermal equilibrium at temperature T_h to another at thermal equilibrium at temperature $T_c < T_h$ without using a third body to absorb the energy mismatch. In our model we won't use two qubits as in Erker et al. but two oscillators. The ladder/battery system in their model will be replaced here with a collective atomic Dicke system (super radiance). A schematic figure is shown in Figure 24. The interaction Hamiltonian in the interaction picture is

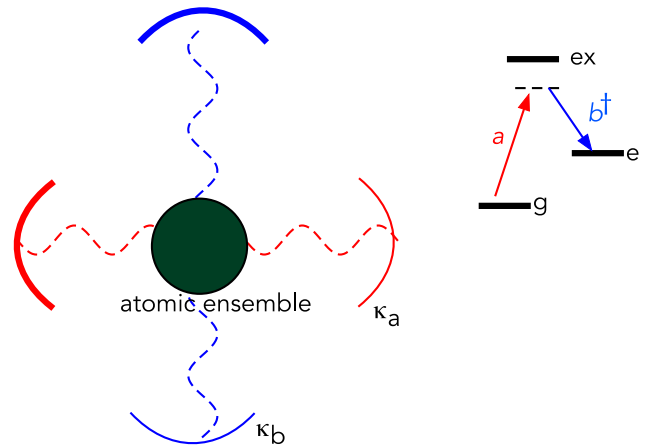$$H_I = \hbar g(ab^\dagger J_+ + a^\dagger b J_-) \qquad (110)$$

Figure 24. Two thermally excited cavities with different frequencies $\omega_a > \omega_b$ are used to excite Raman transitions in an ensemble of atomic systems. Cavity-a is in thermal equilibrium with a heat bath at temperature T_h while cavity-b is in thermal equilibrium with a heat bath at temperature $T_c < T_h$. The frequency difference of the two cavities is resonant with the atomic transition $g \to e$; $\omega_a - \omega_b = \omega_{eg}$.

where $a, a^\dagger, b, b^\dagger$ are bosonic annihilation and creation operators,

$$J_\pm = \sum_{k=1}^N \sigma_\pm^{(j)} \qquad (111)$$

with the raising operator for the j'th atom defined by [30]

$$\sigma_+^{(j)} = |e\rangle_j\langle g| \qquad (112)$$

and we assume Raman resonance $\omega_a - \omega_b = \omega_{eg}$. The atomic system forms a $d = N + 1$ level representation of $su(2)$ with J_x, J_y, J_z defined by

$$J_\pm = \frac{1}{2}(J_x \pm iJ_y) \qquad (113)$$

and

$$J_z = \sum_{k=1}^N (|e\rangle_j\langle e| - |g\rangle_j\langle g|) \qquad (114)$$

The canonical commutation relations using these definitions is

$$[J_x, J_y] = 2iJ_z \qquad (115)$$

$$[J_y, J_z] = 2iJ_x \qquad (116)$$

$$[J_z, J_x] = 2iJ_y \qquad (117)$$

(Note that I am using the definitions in cite [30] so these are not the usual CCRs for su(2).)

The Casimir opreator is

$$J^2 = \left(\frac{1}{2}J_x\right)^2 + \left(\frac{1}{2}J_y\right)^2 + \left(\frac{1}{2}J_z\right)^2 \qquad (118)$$

$$= \frac{1}{2}(J_+J_- + J_-J_+) + \frac{1}{4}J_z^2 \qquad (119)$$

The canonical commutation relations are

$$[J_+, J_-] = J_z \qquad (120)$$

$$[J_z, J_\pm] = \pm J_\pm \qquad (121)$$

We will assume that we remain in the symmetric subspace that is an eigenstate of J^2 with eigenvalue $\frac{N}{2}(\frac{N}{2} + 1)$[31].

The dynamics for the total system is given by the master equation

$$\dot\rho = -ig[ab^\dagger J_+ + a^\dagger bJ_-, \rho] + \kappa_a(N_a + 1)\mathcal{D}[a]\rho$$

$$+ \kappa_a N_a \mathcal{D}[a^\dagger]\rho + \kappa_b(N_b + 1)\mathcal{D}[b]\rho + \kappa_b N_b \mathcal{D}[b^\dagger]\rho$$

$$+ \gamma\mathcal{D}[J_-]\rho \qquad (122)$$

wher N_a, N_n is the mean thermal excitation at frequencies ω_a, ω_b respectively in the thermal baths coupled to the

optical cavities. In the last term we depart from the model of Erker et al. They assumed that emission was only possible from the top weight state of J_z. However our model for decay is the usal Dicke super-radiance model. Indeed a superradiant laser, albeit not based on Raman transitions, has been proposed and demonstrated by [32]. The model thus corresponds to a thermally pumped superradiant system. In this sense it is anlaogous to the optomechnical Mach clock discussed in [33].

Erker et al. [11] consider the case in which the two degrees of freedom coupled to the collective spin remain in thermal equlibrium with their respective heat baths. In the case considered this is equivalent to assuming that the cavities are heavily damped. Note however that [11] consider a very different model for the damping of the collective spin.

An equivalent semiclassical model to the master equation may be given in terms of the quadratic field moments

$$\alpha\beta^* = \langle ab^\dagger\rangle \qquad (123)$$

$$|\alpha|^2 = \langle a^\dagger a\rangle \qquad (124)$$

$$|\beta|^2 = \langle b^\dagger b\rangle \qquad (125)$$

and the scaled atomic moments

$$S = \langle J_-\rangle/N \qquad (126)$$

$$D = \langle J_z\rangle/N \qquad (127)$$

If the cavity decay rates are the largest rates in the system, we can assume the cavity variables are slaved to the atomic variables. The result can be written to order g^2 as

$$\frac{dD}{dt} = 2\Gamma N(N_a - N_b)|S|^2 - 2\gamma N|S|^2 \qquad (128)$$

$$\frac{d|S|^2}{dt} = -N(\Gamma(N_a - N_b) - \gamma)D|S|^2 \qquad (129)$$

where

$$\Gamma = \frac{8g^2}{\kappa_+} \qquad (130)$$

and $\kappa_+ = \kappa_a + \kappa_b$.

This result implies that the atomic master equation in this limit is given by

$$\dot\rho = \Gamma_-\mathcal{D}[J_-]\rho + \Gamma_+\mathcal{D}[J_+]\rho \qquad (131)$$

where

$$\Gamma_- = \Gamma(N_a + 1)N_b + \gamma \qquad (132)$$

$$\Gamma_+ = \Gamma N_a(N_b + 1) \qquad (133)$$

The equations of motion for the atomic moments then obey

$$\frac{dS}{dt} = -\frac{\Gamma_+}{2}\langle J_-J_z\rangle + \frac{\Gamma_-}{2}\langle J_zJ_-\rangle \tag{134}$$

$$\frac{dD}{dt} = 2\Gamma_+\langle J_-J_+\rangle - 2\Gamma_-\langle J_+J_-\rangle \tag{135}$$

Inspection of the adiabatic master equation indicates that the atomic system will be tend to become excited when the rates obey

$$\frac{N_a(N_b+1)}{(N_a+1)N_b + \gamma/\Gamma} > 1 \tag{136}$$

If we ignore spontaneous emission this equation implies that

$$e^{-\beta_a\epsilon_a + \beta_b\epsilon_b} > 1 \tag{137}$$

where $\beta_a = \frac{1}{k_BT_a}, \beta_b = \frac{1}{k_BT_b}, \epsilon_a = \hbar\omega, \epsilon_b = \hbar\omega_b$. It can be easily verified that this defines a 'virtual' oscillator with frequency ω_{eg} at a **negative** effective temperature given by

$$-k_BT_v = \frac{\epsilon_a - \epsilon_b}{\beta\epsilon_a - \beta_b\epsilon_b} \tag{138}$$

which is analogous to the temperature of the virtual qubit defined in Erker et al. [11]

An equivalent stochastic model for the first order field moments can also be defined. The key idea is to represent thermal driving as a complex gaussian white noise process of zero mean and variance determined by the mean photon number in the heat baths attached to each oscillator. This will give a very different perspective to the dynamics of the quadratic moments which correspond to an ensemble average over all such noise realisations. The stochastic simulation corresponds to what could be observed in a single experimental run.

Define the first order moments

$$\alpha = \langle a \rangle \tag{139}$$

$$\beta = \langle b \rangle \tag{140}$$

and factorise all higher order moments. The equations of motion are given by the following Ito system

$$d\alpha = -igN\beta S\,dt - \frac{\kappa_a}{2}\alpha\,dt + \sqrt{\sigma_a/2}\,dW_a(t)) \tag{141}$$

$$d\beta = -igN\alpha S^*\,dt - \frac{\kappa_b}{2}\beta\,dt + \sqrt{\sigma_b/2}\,dW_b(t) \tag{142}$$

$$\dot{S} = (2igN\alpha\beta^* + N\gamma S/2)D \tag{143}$$

$$\dot{D} = -ig(\alpha\beta^*S^* + \alpha\beta S) - 2\gamma N|S|^2 \tag{144}$$

where dW_a, dW_b are the complex valued Wiener process to simulate thermal heating of each cavity mode. The stochastic field equations are precisely what would be obtained if the P-function was used to represent the quantum state of the field.

We recover the deterministic quadratic equations by using the Ito calculus and averaging over the noise, for example, averaging over the noise we find that

$$d|\alpha|^2 = -igN\alpha^*\beta S\,dt + igN\alpha\beta^*S^*\,dt$$
$$- \kappa_a(|\alpha|^2 - \sigma_a)\,dt \tag{145}$$

and we have used the Ito rule $(\sqrt{\sigma_a}\,dW^*(t))(\sqrt{\sigma_a}\,dW(t)) = \sigma_a dt$. Thus we can identify $\sigma_a = N_a$ and likewise $\sigma_b = N_b$.

When the temperature of the bath attached to cavity-a is much higher than for cavity-b a noisy thermal clock results. In Figure 25 I plot $D(t)$ and the real part of $S(t)$ versus time for two sample trajectories. Note that although the period fluctuates from one sample to the next, the system is a good periodic clock. The field radiated by this polarisation will likewise be oscillatory.

5. Fundamental questions relating to clocks and thermodynamics

An understanding of the thermodynamics of clocks suggest novel responses to deep questions in fundamental
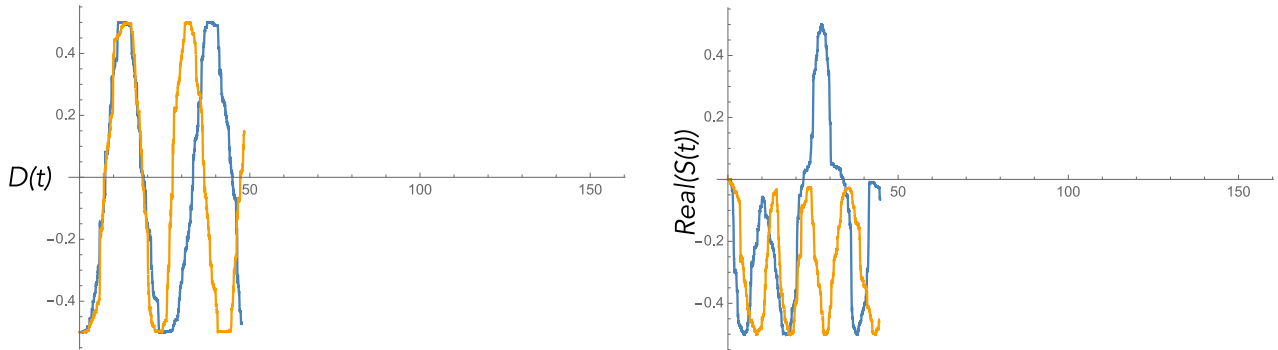

Figure 25. Two sample trajectories for $D(t)$ and $Real[S(t)]$ with $g = 0.2, N = 100.0, \kappa_a = 20.0, \kappa_b = 20.0, \gamma = 20.0, \sigma_a = 50.0, \sigma_b = 0.01$.

physics and philosophy. Mach [23] (see Figure 17) and also Eddington [34] introduced the idea of a thermal or entropy clock to probe the question of the arrow of time. Eddington introduced the idea of an entropy clock in an attempt to penetrate the mystery of perceived time. As he put it [34]

> It seems to me, therefore, that consciousness with its insistence on time's arrow and its rather erratic ideas of time measurement may be guided by entropy-clocks in some portion of the brain. […] Entropy-gradient is then the direct equivalent of the time of consciousness in both its aspects. Duration measured by physical clocks (time-like interval) is only remotely connected.

I think you might agree, having read this far, that his conclusion is misguided: all physical clocks are necessarily irreversible. In this sense all clocks are entropy clocks. The link to consciousness is a more interesting speculation.

Our understanding of time has been enriched by the General Theory of Relativity but Eddington's comment seems to suggest that the time of GR is somehow different to the kind of thing measured by the clocks I have discussed in this paper. This is certainly not the case. The Tolman relations in gravitational thermodynamics points to a deep connection between the time of GR and the thermodynamics of clocks by showing a duality between proper time and temperature. In seeking a quantum theory of gravity the problem of time has led Rovelli [35] to propose the 'thermal time hypothesis'. Thermal clocks give operational significance to this. In the remainder of this paper I will comment on these issues in the light of a deeper understanding of the thermodynamics of clocks.

5.1. General relativity and tolman relations

In his book *Relativity, Thermodynamics and Cosmology* [36] Tolman applied the theory of general relativity to thermodynamical systems. The most significant result from the perspective of this paper is that for a gas in thermal equilibrium and gravitational equilibrium the temperature cannot be uniform and must vary from place to place according to the metric of the relevant space time.

Before presenting the general relativistic case I will begin with the special relativistic case. Consider an observer at rest with respect to a two-level system operating as a thermal clock (see Section 4.4) in contact with a heat bath with a temperature T_0 with respect to that observer. In this case the relation between the estimated elapsed proper time τ and T_0 was seen to be $T_0 \tau = $ *constant*. (Equation (105). For an observer in uniform relative motion at relative velocity v, the elapsed time is dilated to be $t' = \tau / \sqrt{1 - v^2/c^2}$. Given that the physics

of the clock and its interaction with the heat bath are unchanged, we see that for the moving observer the temperature will be estimated to be $T' = T_0 \sqrt{1 - v^2/c^2}$; the correct transformation of temperature in special relativity (see Section 69 of [36]).

Tolman developed a general covariant definition of thermal equilibrium along quite general lines in [36]. I will summarise this result here in Tolman's notation for the case of a sphere of gas held together by gravitational forces and in thermal equilibrium. In this case the general invariant interval can be written as

$$ds^2 = -e^\mu (dr^2 + r^2 \, d\theta^2 + r^2 \sin^2 \theta \, d\phi^2) + e^\nu \, dt^2 \tag{146}$$

where r, θ, ϕ are standard spherical polar coordinates and $\mu = \mu(r), \nu = \nu(r)$. In this case Tolman's condition for thermal equilibrium reduces to

$$\frac{d}{dr} \left(e^{\mu/2} r^2 \frac{d}{dr} \left(\frac{1}{T_0(r)} \right) \right) = \frac{4\pi (\rho_{00} + 3p_0)}{T_0(r)} e^{\mu/2} r^2 \tag{147}$$

at all values r inside the sphere and where $T_0(r)$ is the proper temperature in a thin spherical shell at radius r, while ρ_{00} and p_0 are the mass density and pressure in that shell. Integrating this equation

$$\frac{d \log T_0(r)}{dr} = -\frac{1}{2} \frac{\nu(r)}{dr} \tag{148}$$

equivalently

$$T_0 \sqrt{g_{44}} = \text{constant} \tag{149}$$

where $g_{44} = e^\nu$ is the temporal component of the metric. The same result holds for the case of a sphere of pure black-body radiation. The result Equation (149) also follows by using a two-level thermal clock to measure proper time at radius r, in thermal contact with the local environment at temperature T_0 (Section 4.4).

5.2. Rovelli's thermal time hypothesis

The variable t that appears in the theory of general relativity, like the other coordinates, is arbitrary yet when a physical clock is localised at a space time point it should count events in accordance with this coordinate. That does seem to make the t coordinate special. How do we identify such systems? Rovelli [35, 37] has proposed the 'thermal time hypothesis' to address this question. The essential idea is a link between a local statistical state and a dynamical flow on physical quantities. This breaks the relationship between the space time metric and temporality and thus looks promising for a concept of time in quantum gravity. The thermodynamics of the machines we call clocks gives a concrete manifestation of this idea.

As discussed in this paper, periodic clocks are driven, non equilibrium dissipative systems. Non periodic clocks (thermal clocks) are systems driven from thermal equilibrium by measurement induced entropy reduction. In both cases they require a source of free energy to operate; work in the case of periodic clocks and accurate measurement in the case of non periodic clocks. All clocks are irreversible systems.

In the case of thermal clocks the steady state of the unconditional (non measured) dynamics is given by the Gibbs-Boltzmann distribution

$$\rho_\beta = Z^{-1} e^{-\beta \hat{H}} \tag{150}$$

where $\beta = 1/k_B T$ and $\hat{H}$ is the Hamiltonian operator. (I will assume quantum physics here). Proceeding formally for now, take the log of ρ as a definition of the Hamiltonian up to a multiplicative factor

$$\beta \hat{H} = \ln(\rho_\beta) \tag{151}$$

The thermal flow of an observable represented by a hermitian operator $\hat{A}$ defined by $\alpha_\tau^\rho(\hat{A})$ satisfies

$$\frac{d\alpha_\tau^\rho(\hat{A})}{d\tau} = -\frac{i}{\hbar}[\log \rho, \hat{A}] \tag{152}$$

The thermal time of an equilibrium state τ at temperature T and the Schroedinger quantum mechanical time t are related by

$$\frac{d}{d\tau} = \beta \frac{d}{dt} \tag{153}$$

Rovelli and Smerlak [37] interpret β as the 'speed' of thermal time; a rather novel reinterpretation of temperature.

We can obtain a similar result by assuming that the history of thermal jumps t_n in the thermal clock index the state of every other local system, In other words the state of a system is parameterised in terms of the stochastic process $\rho_S(t_n)$. One way to think of this is that we only ever measure the system state at the times t_n. In [38] I showed how this kind of stochastic time can be formulated as a dynamical flow in terms of local lab time. If we average over the stochastic history of times, the dynamics can be written in Schroedinger mechanical time as

$$\frac{d\rho_s}{dt} = \gamma \bar{n} \left(\exp\left[-i\frac{\hat{H}_s}{\hbar \gamma \bar{n}}\right] \rho_s \exp\left[i\frac{\hat{H}_s}{\hbar \gamma \bar{n}}\right] - \rho_s \right) \tag{154}$$

At high temperatures $\bar{n} = (\beta \epsilon)^{-1}$ where ϵ is the energy difference between the two states of the thermal clock. We then find that in the limit $\gamma \to \infty$, the good clock limit, the dynamics may be approximated by

$$\frac{d\rho_s}{d\tau} = \frac{-i}{\hbar}[\ln \rho_{s,\beta}, \rho_s] \tag{155}$$

where $\rho_{s,\beta}$ is the steady state of the system itself at thermal equilibrium with the same environment as that of the clock. This is analogous to Rovelli's thermal time flow differential map. It must be admitted however that the first order corrections to this equation in γ^{-1} lead to intrinsic decoherence in all quantum dynamics [38].

Rovelli actually makes a more general hypothesis: any stationary state ρ can be used to define a temporal flow. I expect that this corresponds to the more general case of irreversible periodic clocks. It is interesting to note that the stationary solutions of Equation (154) are diagonal in the eigenstates of the system Hamiltonian. This would justify applying the thermal time hypothesis in the more general form.

6. Conclusion

All physical clocks are open non equilibrium systems constrained by thermodynamics and necessarily irreversible. All clocks are physical systems pushed away from thermal equilibrium thereby increasing their free energy. In the case of periodic clocks this is achieved by an external mechanism doing work on the system, for example a battery. In the case of non periodic 'thermal clocks' it is achieved by decreasing entropy through thermal or chemical potential gradients or, more interestingly, through measurement.

As dissipative systems, all clocks are subject to noise which limits their performance. For classical clocks the source of noise is thermal and goes to zero with temperature. Thermal noise leads to phase diffusion when clocks are running on large amplitude limit cycles. In the case of quantum clocks noise remains even at zero temperature due to, for example, spontaneous emission or quantum tunnelling. By using a range of examples both classical and quantum I have shown that the thermodynamic constraints require good clocks to dissipate large amounts of energy.

An understanding of the thermodynamic limits of clocks gives important insights into the nature of physical time. I have shown how, for example, thermal clocks can be used to give a physical realisation of Rovelli's thermal time hypothesis.

Our understanding of clock performance is crucial for emerging quantum technologies [39]. Indeed ideas from quantum information, such as gate fidelity, may provide even better measures of clock performance than traditional metrics. As our understanding of the links between thermodynamics and quantum information increases we will be led to novel kinds of clocks that exceed the already incredible performance of current atomic clocks.

Disclosure statement

No potential conflict of interest was reported by the author.

Notes on contributor

Gerard Milburn is a Chief Investigator in the Centre for Engineered Quantum Systems at The University of Queensland, Australia. He obtained a PhD under the supervision of Dan Walls at The University of Waikato in 1982. He has worked in many fields of theoretical physics including quantum optics, quantum measurement and control and quantum information. His is currently investigating how engineered quantum systems can enhance machine learning. He is a Fellow of the Australian Academy of Science and the Royal Society of London.

References

[1] Woods MP. Autonomous ticking clocks from axiomatic principles. arXiv:2005.04628. 2020.

[2] Jesperson J, Fitz-Randolph J. From sundials to atomic clocks: understanding time and frequency. NIST Monograph. 1999;155:1–306.

[3] Ford GW. The fluctuation dissipation theorem. Contemp Phys. 2017;58:244.

[4] Du R, Xie L. The mechanics of mechanical watches and clocks. Berlin: Springer; 2013.

[5] For an animation of the wheel and anchor mechanism see: https://woosterphysicists.scotblogs.wooster.edu/2016/01/10/ticktock-deadbeat-escapement/.

[6] Hoyng P. Dynamics and performance of clock pendulums. Am J Phys. 2014;82:1053.

[7] Weiss U. Quantum dissipative systems. Singapore: World Scientific; 2012.

[8] Gardiner CW. Handbook of stochastic processes for physics chemistry and the natural sciences. Berlin: Springer; 1983.

[9] Zhu W-Q, Yu J-S. On the response of the Van Der Pol oscillator to white noise excitation. J Sound Vib. 1987;17:421.

[10] Rutman J. Characterisation of phase and frequency instabilities in precision frequerncy sources: fifteen years of progress. Proc IEEE. 1978;66:1048.

[11] Erker P, Mitchison MT, Silva R, et al. Autonomous quantum clocks: does thermodynamics limit our ability to measure time? Phys Rev X. 2017;7:031022.

[12] Marrison A. The evolution of the quartz crystal clock. Bell Syst Tech J. 1948;XXVII:510–588.

[13] Bruce McNamara B, Kurt Wiesenfeld K. Theory of stochastic resonance. Phys Rev A. 1989;39:4854.

[14] Levine J. Introduction to time and frequency metrology. Rev Sci Instrum. 1999;70(6):2567–2596.

[15] Wiseman HM. Optical coherence and teleportation: why a laser is a clock, and not a quantum channel. Proceedings Volume 5111, Fluctuations and Noise in Photonics and Quantum Optics; SPIE. 2003. Available from: https://doi.org/10.1117/12.497090.

[16] Wiseman HM. Light amplification without stimulated emission: beyond the standard quantum limit to the laser linewidth. Phys Rev A. 1999;60:4083.

[17] Wiseman HM. Stochastic quantum dynamics of a continuously monitored laser. Phys Rev A. 1993;47:5180.

[18] Walls DF, Milburn GJ. Quantum optics. 2nd ed. Berlin: Springer-Verlag; 2008.

[19] Wiseman HM, Milburn GJ. Quantum measurement and control. Cambridge: Cambridge University Press; 2010.

[20] Park H, Park J, Lim AK, et al. Nanomechanical oscillations in a single-C_{60} transistor. Nat Lond. 2000;407:57.

[21] Utami DW, Goan HS, Holmes CA, et al. Quantum noise in the electromechanical shuttle: quantum master equation treatment. Phys Rev B. 2006;74:014303.

[22] Buonomano D. Your brain is a time machine: the neuroscience and physics of time. New York: W. W. Norton; 2017.

[23] Mach E. Knowledge and Error, pp 339. (D. Reidel Pub. Co, Springer Netherlands, Reidel, 1976); J. Bradley, Mach's Philosophy of Science, (The Athlone Press, The University of London, 1971).

[24] Pearson A, Guryanova Y, Erker P, et al. Measuring the thermodynamic cost of timekeeping. arXiv:2006.08670. 2020.

[25] Tanaka S. Appearance of thermal time. arXiv:2006.08932. 2020.

[26] Vijay R, Slichter DH, Siddiqi I. Observation of quantum jumps in a superconducting artificial atom. Phys Rev Lett. 2011;106:110502.

[27] Koch J, Terri MY, Gambetta J, et al. Charge-insensitive qubit design derived from the Cooper pair box. Phys Rev A. 2007;76:042319.

[28] Johnson BR, Reed MD, Houck AA, et al. Quantum nondemolition detection of single microwave photons in a circuit. Nat Phys. 2010;6:663.

[29] Mitchison MT. Quantum thermal absorption machines: refrigerators, engines and clocks. Contemp Phys. 2019; 60:164. Available from: https://doi.org/10.1080/00107514.2019.1631555.

[30] Carmichael HJ. Statistical methods in quantum optics 1. Berlin: Springer; 1999.

[31] Arrechi FT, Courtens E. Cooperative phenomena in resonant electromagnetic propagation. Phys Rev A. 1970;2:1730.

[32] Meiser D, Ye J, Carlson DR, et al. Prospects for a mHz-linewidth laser. 10.1103/PhysRevLett.102.163601.

[33] Milburn GJ, Milburn TJ. A quantum optomechanical Mach clock. arXiv:1708.02369.

[34] Eddington A. The nature of the physical world. Cambridge: Cambridge University Press; 1948.

[35] Rovelli C. Quantum gravity. Cambridge: Cambridge University Press; 2004.

[36] Tolman RC. Relativity, thermodynamics and cosmology. New York: Dover; 1934.

[37] Rovelli C, Smerlak M. Thermal time and the Tolman-Ehrenfest effect: temperature as the speed of time. Class Quant Grav. 2011;28:075007.

[38] Milburn GJ. Intrinsic decoherence. Phys Rev A. 1991; 44:5401.

[39] Ball H, Oliver WD, Biercuk MJ. The role of master clock stability in quantum information processing. npj Quant Inform. 2017;2:16033. doi:10.1038/npjqi.2016.33.